Research Square

Preprints are preliminary reports that have not undergone peer review.
They should not be considered conclusive, used to inform clinical practice,
or referenced by the media as validated information.

Design, Economics Evaluation, and Simulation of Proposed Independent Solar Photovoltaics System for the Electrification of Itunta Village

Igwe Johnson Eze

igwe.johnson@mouau.edu.ng

Michael Okpara University of Agriculture

Anyaele Jude Uwakwe

Michael Okpara University of Agriculture

Emmanuel Ebube Eze

Michael Okpara University of Agriculture

Research Article

Keywords: rural electrification, battery optimization, stochastic reliability, load aggregation, life-cycle costing, sensitivity analysis

Posted Date: November 25th, 2026

DOI: https://doi.org/10.21203/rs.3.rs-11420513/v1

License: This work is licensed under a Creative Commons Attribution 4.0 International License.
Read Full License

Additional Declarations: No competing interests reported.

DESIGN, ECONOMICS EVALUATION, AND SIMULATION OF PROPOSED INDEPENDENT SOLAR PHOTOVOLTAICS SYSTEM FOR THE ELECTRIFICATION OF ITUNTA VILLAGE

Igwe Johnson Eze[1]*, Anyaele Jude Uwakwe[1], Emmanuel Ebube Eze[2]
[1]Mechanical Engineering Department, Michael Okpara University of Agriculture, Umudike, Abia State, Nigeria.
[2]Department of Civil Engineering, Michael Okpara University of Agriculture, Umudike, Abia State, Nigeria
Email: igwe.johnson@mouau.edu.ng[1]*;
judeuwakwe.ju@gmail.com[2];emmanuelebube450@gmail.com[3]

Abstract

Access to reliable electricity remains a major challenge in rural Nigeria, where grid extension and diesel generation are costly and uncertain. This study develops a field-informed techno-economic and long-term reliability framework for a standalone photovoltaic mini-grid serving Itunta Village. The load assessment covered all 136 accessible households and community facilities, while solar-resource characterization used PVGIS data for 2005–2025. The baseline demand was 806.16 kWh/day, and the conservative design comprised 401 SunPower 435 W modules (174.32 kWp) and 896 lithium-ion battery units. The array produced an average daily yield of 890.41 kWh/day, with seasonal output decreasing to approximately 660 kWh/day in July. The scientific contribution is the integration of field-based load aggregation, stochastic resource variation, battery cost–reliability optimization, lifecycle costing, and 25-year adequacy projection within one reproducible case-study framework. A technical sensitivity screen showed that a 10% reduction in irradiance removes the average energy margin, while a 10% increase in load nearly exhausts it, demonstrating the importance of uncertainty-aware sizing. The optimized one-day-autonomy configuration reduced the battery bank to 598 units and the battery cost to approximately ₦344.45 million while maintaining 95.974% reliability and an LPSP of 0.040256. The simplified LCOE was ₦89.91/kWh, whereas the discounted lifecycle LCOE was ₦358.63/kWh and the corresponding net present cost was approximately ₦1.02 billion. Long-term simulation showed that reliability decreases from 91.82% in Year 1 to 54.26% in Year 25 under 2% annual load growth, with a substantially faster decline under 5% growth. The results indicate that the system is technically feasible for present demand but requires modular implementation, disciplined battery management, and planned mid-life expansion to remain reliable over its full service life.

Keywords: rural electrification; battery optimization; stochastic reliability; load aggregation; life-cycle costing; sensitivity analysis.

1. Introduction

Access to reliable electricity remains a major driver of socio-economic development, yet a large portion of the population in Sub-Saharan Africa still lacks dependable electricity supply. Traditional grid extension to remote rural settlements is often constrained by high capital cost, difficult terrain and low economic return, making decentralized renewable energy systems increasingly attractive for rural electrification. In this context, solar photovoltaic (PV) mini-grids have emerged as one of the most practical and cost-effective options for supplying clean electricity to off-grid communities (Cyril et al., 2024; Mbinkar et al., 2021; Wassie & Adaramola, 2021). Rural PV electrification is commonly implemented through standalone

systems or mini-grid configurations. Standalone PV systems are suitable for isolated loads or single households while mini-grids are more appropriate for clustered communities where diverse demand can be served more efficiently through a shared generation and distribution network. Prior studies have demonstrated the technical viability of standalone rural PV systems and community-scale mini-grids in different settings (Fakher Alfahed et al., 2019; Al-Shetwi, 2016; Mbinkar et al., 2021). However, many existing studies emphasize component sizing or short-term feasibility while fewer combine field-based load assessment, long-term resource variability, stochastic reliability analysis, and lifecycle economic evaluation within one site-specific framework.

The design of an independent solar PV system requires accurate determination of the load profile, solar resource availability, storage capacity, and power electronics configuration. The PV array, battery bank, charge controller, and inverter must be selected in a coordinated manner to ensure reliability, energy balance, and acceptable system losses (Li et al., 2024; Mbinkar et al., 2021). In addition to basic sizing, robust design increasingly requires consideration of seasonal irradiance variation, temperature effects, component degradation, and changing demand over time. These factors are especially important in rural electrification projects, where under-sizing can lead to supply inadequacy, while excessive oversizing can make the system economically unattractive.

Economic assessment is equally important because high initial capital cost remains a major barrier to PV deployment in rural areas. Life-cycle cost, levelized cost of electricity, replacement cost, and operation and maintenance cost are therefore essential indicators for judging project viability (Mbinkar et al., 2021; Al-Shetwi, 2016; Uwibambe, 2017). In addition, rural electrification projects should not be evaluated only at the point of installation; they must also be examined over their operating life to determine whether reliability remains acceptable as the system ages and local demand grows. This long-term perspective is particularly relevant for isolated communities where future load growth may arise from improved appliance ownership, small businesses and productive energy use.

The present study contributes new knowledge by developing a site-specific techno-economic and reliability framework for Itunta Village, Abia State, based on field-surveyed household demand, long-term PVGIS climate data, MATLAB-based stochastic simulation, Monte Carlo variability, PV degradation, battery aging and load growth modelling. Unlike studies that stop at initial sizing, this work examines how the proposed system performs over a 25-year horizon and shows how reliability changes as environmental conditions and demand evolve. The study therefore provides an integrated basis for evaluating not only whether the system can meet present demand but also how long it can sustain acceptable service before expansion becomes necessary.

Accordingly, this research is novel in its combined treatment of community-level load assessment, long-term resource characterization, stochastic reliability projection and economic appraisal for a rural Nigerian mini-grid. The findings offer a practical design reference for similar off-grid communities and help define which aspects of the system are site-specific and which may be generalized to other rural electrification projects. The study is therefore relevant to researchers, practitioners and policymakers seeking technically sound and economically defensible pathways for decentralized rural electrification in Sub-Saharan Africa.

1.1 Critical Literature Review

Recent rural-electrification research confirms that photovoltaic mini-grids can provide technically viable and socially beneficial electricity services, but the analytical emphasis differs widely across studies. Mbinkar et al. (2021) and Al-Shetwi (2016) demonstrate the practicality of PV mini-grid and standalone designs, whereas more recent Nigerian studies increasingly use software-based optimization to compare hybrid configurations and lifecycle costs. For example, Lewis et al. (2024) used HOMER to optimize a PV–battery–generator microgrid for a 610 kWh/day rural load in northeast Nigeria and reported an LCOE of 0.0927 USD/kWh and an NPC of USD 266,709. Adefarati et al. (2024) likewise emphasized multi-constraint techno-economic optimization for a standalone PV–diesel–battery system. These studies establish the value of economic optimization, but hybrid backup generation can mask the long-term adequacy limitations of a PV-only system.

Uncertainty treatment is another important research direction. Quiles-Cucarella et al. (2023) combined sequential Monte Carlo simulation with particle-swarm optimization to size standalone PV systems while explicitly representing variability in irradiance and demand. Their work demonstrates why average-value sizing should be supplemented with chronological reliability analysis. Battery aging also cannot be represented by a universal annual percentage alone: Luo et al. (2023) showed that temperature, depth of discharge, state-of-charge window, and charge/discharge rate materially change lithium-ion degradation mechanisms. At the implementation level, Carabajal et al. (2024) documented substantial social and economic benefits from solar mini-grid access in Kenya and Nigeria, reinforcing the need to evaluate not only initial technical feasibility but also durable service quality and affordability.

The literature therefore reveals four recurring gaps: limited integration of field-surveyed community demand with long-term stochastic reliability; insufficient treatment of load growth and interannual resource variability; incomplete reporting of storage replacement and lifecycle cost; and weak translation of calculated component sizes into practical installation, safety, maintenance, and expansion plans. The present study is structured to address these gaps for a rural Nigerian community while clearly distinguishing the site-specific numerical results from the transferable analytical framework.

1.2 Research Gap and Original Scientific Contribution

The original contribution of this work is not a new PV sizing equation; rather, it is an integrated decision framework that links field-based demand characterization, long-term PVGIS resource data, stochastic daily simulation, storage optimization, lifecycle economics, and expansion planning. The study advances previous rural PV case studies in four specific ways: (i) it quantifies how the initially adequate system loses reliability over a 25-year horizon under competing PV degradation and load-growth trends; (ii) it identifies a cost–reliability storage sweet spot rather than accepting the conventional autonomy assumption as automatically optimal; (iii) it reports simplified and discounted economic indicators, including replacement burden and NPC; and (iv) it converts the calculated capacities into a modular implementation, maintenance, safety, and replacement strategy. This combination provides a replicable basis for determining when a rural PV mini-grid is adequate at commissioning and when reinforcement becomes necessary.

2. Materials and Methods

2.1 Research design

This study employed an engineering-based techno-economic feasibility framework that combined quantitative analysis, component sizing, lifecycle costing, and chronological system simulation. Figure 1 summarizes the principal methodological steps undertaken in the study.

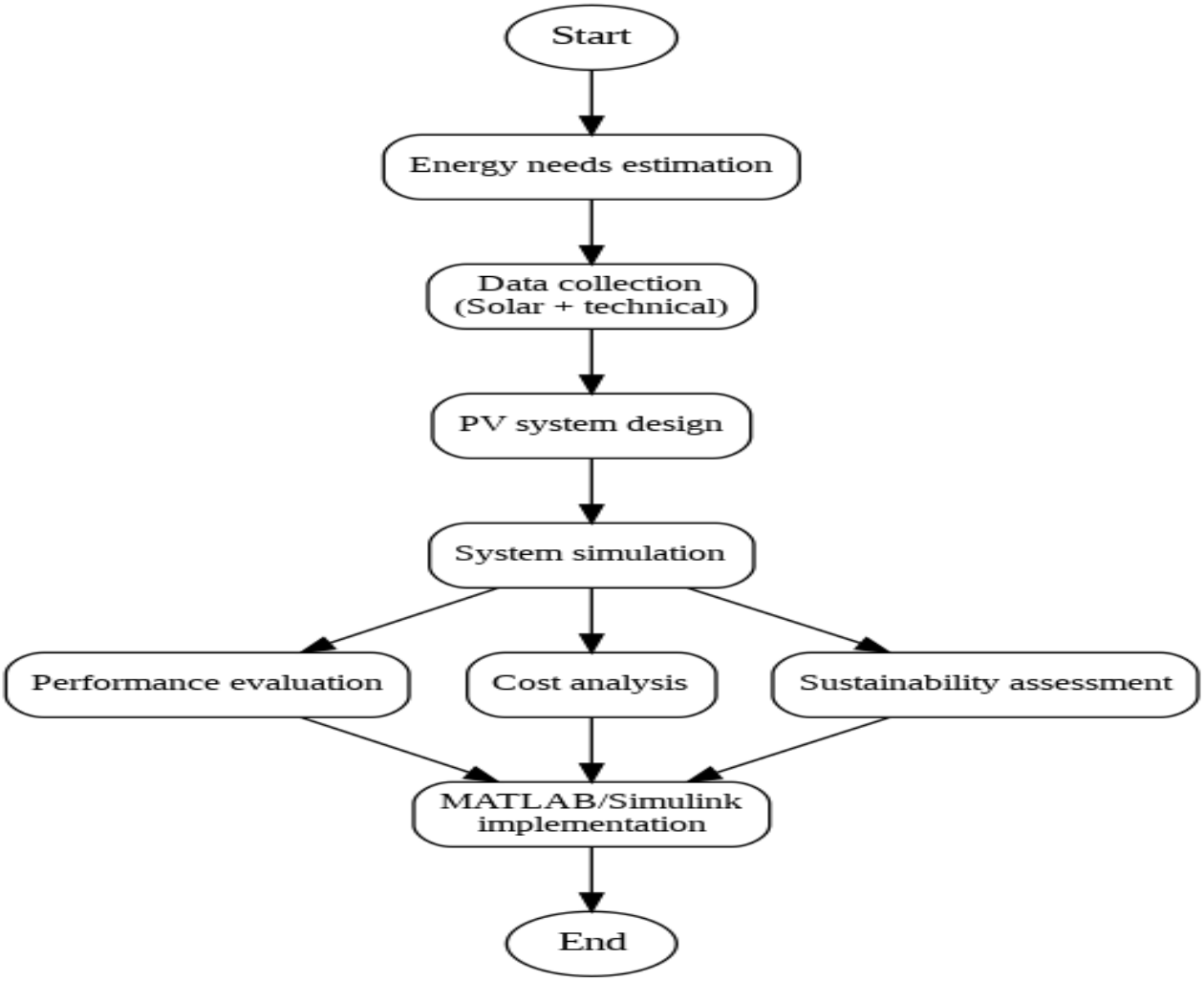

Figure 1: Methodology flow chart

2.2 Description of the study area (Itunta Village, Abia State)

Itunta Village is a rural community in the Ikwuano Local Government Area of Abia State, southeastern Nigeria. The village has limited access to reliable grid electricity and currently depends largely on kerosene lamps, firewood and small petrol generators for domestic and small business energy needs. The community experiences relatively favorable solar irradiation with average daily solar radiation estimated at approximately 5.1–5.8 kWh/m²/day based on PVGIS data and cross-checked using local data. The settlement includes residential households, small shops, schools and a health center, each with distinct electricity demand patterns. These mixed-use loads make Itunta Village appropriate for a

community-scale solar mini-grid assessment. The location of the village and the proposed installation zone is shown in Figure 2.

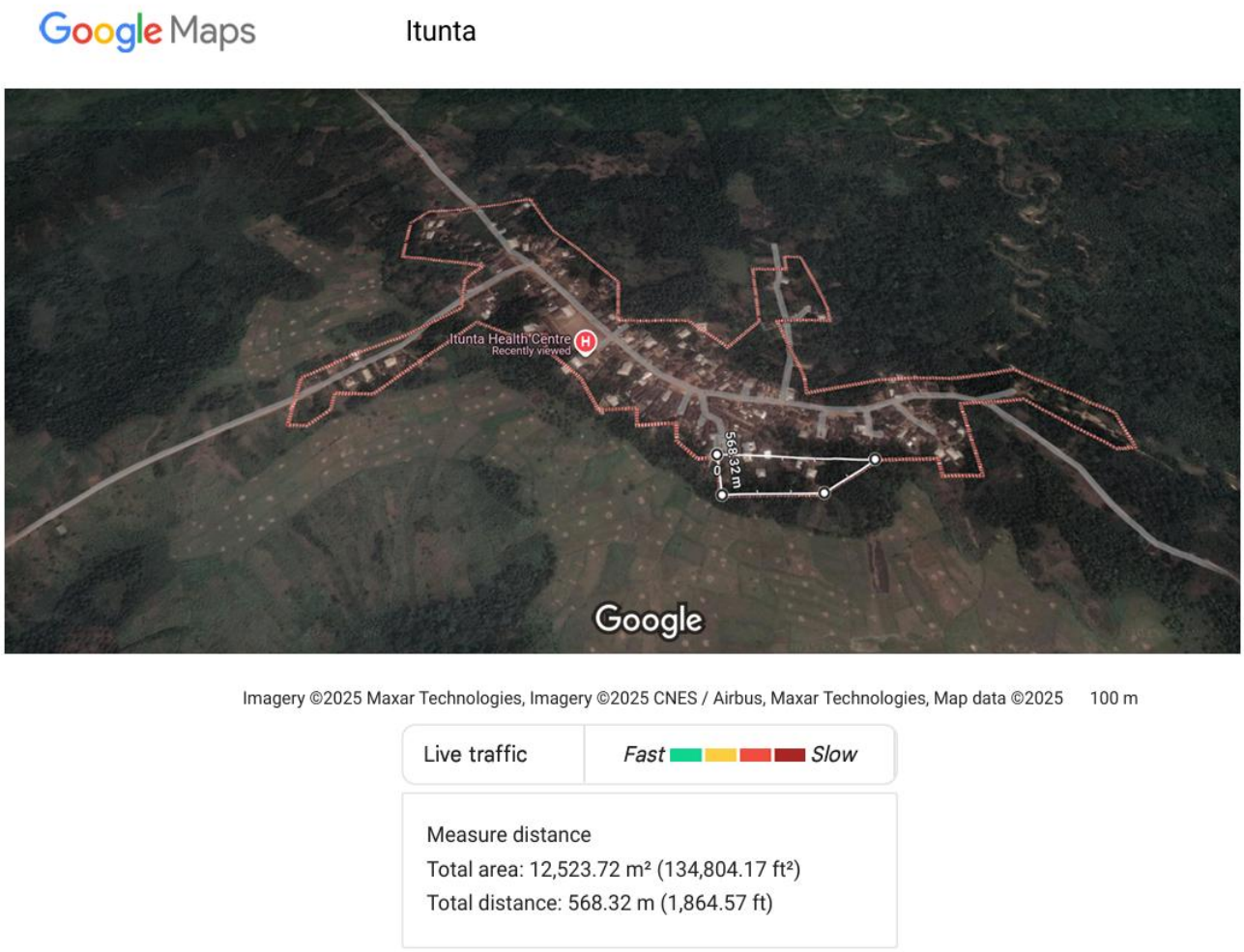

Figure 2: Itunta map showing the proposed installation zone

2.3 Preliminary Activities and Data Collection Procedure

A preliminary visit was conducted to Itunta Village after obtaining permission from the community leadership through a formal letter submitted to the Town Union authorities. The visit provided direct information on the community's energy requirements, site conditions, settlement pattern and socio-economic characteristics. Community mapping was carried out and key facilities were identified. The existing energy sources such as kerosene lamps and generators were documented to support accurate load estimation and system design.

Table 1 presents the daily electrical load profile developed from primary data obtained through on-site household surveys, appliance inspection, interviews with residents and business owners, and direct observation of usage patterns. The survey followed a census-of-accessible-households approach rather than random sampling: all 136 homes that could be reached during the field investigation were included, together with the principal community and small-commercial loads. For each load, the research team recorded appliance type, quantity, nameplate power, typical operating period, and average daily operating hours. Interview responses were cross-checked against visible appliances and reported community routines to reduce recall error. The resulting inventory therefore represents the accessible

occupied households at the time of the survey, but it is not a probability sample of future households or seasonal residents.

$$E_d = \sum_{j=i}^{n} E_j \quad (1)$$

The total daily energy demand is the sum of the daily energy contribution of each appliance class. The baseline profile was constructed deterministically from the average daily operating hours observed during the survey, while approximate hourly usage windows were assigned to lighting, fans, refrigerators, televisions, pumps, and productive-use loads. Because interval meters were not available, coincidence and operating-hour estimates remain uncertain. To make this limitation explicit, the analysis includes ±10% load-demand sensitivity cases and a combined adverse case with higher demand and lower irradiance. Seasonal household-consumption changes were not separately measured; consequently, the measured average profile is treated as the commissioning-year baseline rather than a permanent forecast. This limitation is considered in the load-growth and uncertainty analyses.

Secondary solar irradiance and temperature records for 2005–2025 were obtained from PVGIS and cross-checked against available local values from the meteorological unit of the National Root Crops Research Institute, Umudike. Monthly seasonality, interannual variation, and stochastic daily perturbations were retained for reliability analysis rather than replacing the entire record with one annual average. The long-term dataset was also used to define low-resource and high-resource sensitivity cases so that the design could be tested against rainy-season stress and plausible year-to-year fluctuations.

Technical specifications and cost data for the system components were sourced from manufacturers' datasheets and publicly available documentation. These data were combined with the field survey results and solar resource data to support system sizing, performance evaluation, and techno-economic analysis.

2.4 Solar panel and module estimation

The total electricity demand of Itunta Village, obtained from the field-based load assessment, was used as the basis for sizing the photovoltaic array. To avoid undersizing during the worst solar months and to support battery charging requirements, the PV system was sized using a loss-inclusive design equation as given by Bhatia (2008) and Babatunde et al., (2019).

$$Module\ Peak\ wattage\ (Wp) = \frac{\Sigma(Daily\ Energy\ Demand\ Wh)}{PSH \times \eta_b} \quad (2)$$

where $\Sigma\,(Daily\ Energy\ Demand\ Wh)$ is the daily energy demand, PSH is the peak sunshine hours, and η_b is the overall system efficiency factor which includes temperature, wiring, inverter, controller and mismatch losses.

The number of modules required was then obtained as:

$$Number\ of\ Modules\ or\ panels\ =\ N_{P2} = \frac{SPV\ Module\ Wattage\ Estimation}{Value\ of\ Each\ Panel} \quad (3)$$

A SunPower 435 W module was selected for the design because of its high conversion efficiency and reduced land requirement. The PV array was therefore sized not only to satisfy average daily demand but also to maintain charging reserve. This improves reliability during low-irradiance periods. Any surplus generation is first directed to battery charging, then to reserve capacity for deficit periods and finally to controllable or productive loads where such loads are available.

2.5 Battery sizing

Battery storage was sized to provide three days of autonomy and to maintain supply continuity during periods of reduced solar availability. The required usable storage energy was estimated from the daily demand and autonomy requirement as given by Diyoke et al. (2023) and Chanchangi et al., (2023). The nominal storage capacity was then derived by accounting for depth of discharge and round-trip battery efficiency.

$$E_{bat,usable} = Ed \times A \tag{4}$$

$$E_{bat,nominal} = \frac{E_{bat,usable}}{DOD \times \eta_{rt}} \tag{5}$$

where A is the autonomy period in days, DOD is the allowable depth of discharge, and η_{rt} is the battery round-trip efficiency. The battery bank was therefore treated as a modular lithium-ion storage system rather than a single oversized unit. For practical implementation, the storage subsystem is arranged in series-parallel strings to match the selected DC bus voltage. The thermal control, accessibility and protection are considered in the physical layout.

2.6 The charge controller selection

The charge controller capacity was determined as outlined by Chetan (2014) and Chandramouli et al., (2019) from the aggregate PV array current and the selected DC bus voltage. To improve practical implementation and reduce excessive current, the design was to use a higher-voltage modular DC architecture rather than a single low-voltage bus for the full village load.

$$SCC = \frac{P_{PV}}{V_{bus}} \tag{6}$$

where P_{PV} is the total PV array power and V_{bus} is the nominal DC bus voltage.

Multiple MPPT charge controllers were selected in parallel to manage subarray charging, improve tracking efficiency, and allow current distribution across modular sections of the system.

2.7 Inverter sizing

The inverter capacity was sized from findings drawn from Leonics (2009) and Debnath & Chatterjee, (2016). to accommodate the peak connected load with an additional design margin to support transient and startup conditions.

$$P_{inv} = 1.25 \times P_{load,peak} \tag{7}$$

Where$P_{load,peak}$ is the maximum concurrent demand from household and community appliances.

The inverter arrangement was treated as a modular AC conversion system supplying a 230 V AC distribution network. This ensures compatibility with domestic and community-level appliances while maintaining stable output during fluctuations in solar input and battery discharge.

2.8 Maximum direct/alternating current and voltage of wire

The maximum current in the DC and AC sections of the system was determined using the system voltage architecture and the rated load power. Conductor sizing was then guided by allowable current density, voltage-drop limits, and protection requirements (Chidiebere et al., 2021).

$$IDC = \frac{P_{DC}}{V_{bus}} \tag{8}$$

$$I_{AC} = \frac{P_{AC}}{V_{AC}} \tag{9}$$

where P_{DC} and P_{AC} are the relevant DC and AC power levels, while V_{bus} and V_{AC} are the DC bus and AC distribution voltages respectively.

The system is structured around modular subarrays and a practical voltage level that supports safe wiring, protection, and acceptable losses.

2.9 Solar performance ratio

The Solar Performance Ratio (PR) was used to evaluate how effectively the photovoltaic system converts available solar resource into useful output after accounting for system losses. Solar Performance Ratio (SPR %) according to Jara *et al.,* (2020), and Das & Frank (2019) is stated in equation (9).

$$PR = \frac{E_{actual}}{E_{theoretical}} \times 100 \tag{10}$$

where E_{actual} is the measured or simulated delivered energy and $E_{theoretical}$ is the reference energy available under ideal conditions. The loss terms considered in the analysis include temperature losses, inverter losses, controller losses, wiring losses, mismatch losses and soiling losses. This makes the PR more representative of field operating conditions and avoids overestimating system performance.

2.10 System Configuration and Wiring Methodology

The system configuration was defined using a modular series-parallel arrangement to ensure safe and efficient operation. The design adopts a higher-voltage DC storage and charging architecture with the PV field divided into subarrays feeding separate MPPT controller banks. This reduces current stress, improves protection coordination and simplifies maintenance. PV modules are connected in series to achieve the required charging voltage and grouped in parallel to satisfy the total power requirement. The battery bank is also configured in series-parallel strings to match the nominal DC bus voltage while achieving the needed storage capacity. The inverter stage converts the stored DC power to 230 V AC for household and community use. The wiring methodology also includes: DC isolators, string fuses, surge protection devices, proper earthing, cable sizing based on current and voltage-drop limits and feeder segregation for safe distribution. This configuration provides a practical basis for the design, installation and operation of the mini-grid while addressing the feasibility concerns raised during peer review.

2.11 Economic and Performance Evaluation Metrics

The economic viability and technical resilience of the Itunta Village solar mini-grid are evaluated using the following mathematical models.

a. System Capital Expenditure (CAPEX)

The total initial investment cost (C_{total}) is the summation of the individual costs of the solar array, battery storage, power electronics, and the balance of system (BoS) components (Wassie, & Adaramola, 2021; Ngo).

$$C_{total} = (N_p \cdot C_p) + (N_b \cdot C_b) + (N_{cc} \cdot C_{cc}) + (N_{inv} \cdot C_{inv}) + C_{BoS} \quad (11)$$

Where:

- $N_p, N_b = Total\ number\ of\ PV\ panels\ and\ batteries, respectively.$
- $C_p, C_b = Unit\ cost\ of\ a\ single\ PV\ panel\ and\ battery, respectively.$
- $N_{cc}, N_{inv} = Number\ of\ charge\ controllers\ and\ inverter\ units.$
- $C_{BoS} = Costs\ associated\ with\ installation, mounting\ structures, and\ cabling.$

b. Levelized Cost of Electricity (LCOE)

The LCOE is the fundamental metric used to compare the cost of solar generation against the local utility or diesel rates. It represents the average cost per kWh of useful energy produced over the system's life cycle (n).

$$LCOE = \frac{C_{total} + \sum_{t=1}^{n} \frac{M_t}{(1+r)^t}}{\sum_{t=1}^{n} \frac{E_t}{(1+r)^t}} \quad (12)$$

For the simplified linear model used in this analysis (where r is the discount rate and M_t is annual maintenance):

$$\text{LCOE} = \frac{CAPEX + OPEX_{total}}{E_{lifetime}} \quad (13)$$

Where:

- $E_{lifetime} = Total\ energy\ generated\ over\ 25\ years\ (kWh).$
- $OPEX_{total} = Total\ operating\ and\ maintenance\ costs\ over\ the\ system\ life.$

c. Simple Payback Period (SPP)

The payback period determines the time required to recover the initial investment through the displacement of diesel generation costs.

$$SPP = \frac{C_{total}}{S_{annual} - OPEX_{annual}} \quad (14)$$

Where:

- $S_{annual} = Annual\ savings\ (Annual\ Energy\ Yield \times Cost\ of\ Diesel\ per\ kWh).$

- $OPEX_{annual} = Annual\ operation\ and\ maintenance$ costs.

d. Energy Payback Time (EPBT)

The EPBT evaluates the environmental sustainability by calculating how many years the system must operate to repay the energy used during its manufacture (E_{mat}).

$$EPBT = \frac{E_{mat} + E_{inst} + E_{trans}}{E_{annual} - E_{oper}} \quad (15)$$

Where:

- $E_{annual} = Annual\ energy\ generated\ by\ the\ system.$
- $E_{mat} = Energy\ embodied\ in\ the\ solar\ panels\ and\ components.$

2.12 Simulation-Based Reliability Modelling Methodology

A simulation-based research methodology was implemented in the MATLAB environment to evaluate the long-term performance and reliability of the proposed solar photovoltaic mini-grid. The model integrates seasonal solar resource modelling, stochastic daily variability, PV degradation, load growth, battery state-of-charge (SoC) dynamics and Response Surface Methodology (RSM) to quantify the sensitivity of PV output to irradiance and temperature. The simulation was run over a 25-year daily time-step horizon, giving a total of approximately:

$$N = 25 \times 365.25 \approx 9131\ days \quad (16)$$

This time resolution captures both short-term daily fluctuations and long-term system ageing trends.

2.12.1 Seasonal Solar Resource Modelling

The baseline solar output was represented using a harmonic seasonal cycle calibrated to Nigerian climatic conditions. The seasonal daily yield was defined as:

$$P_{season}(t) = P_{mean} - \text{Acos}\left(\frac{2\pi(t - t_0)}{365.25}\right) \quad (17)$$

where:

- P_{mean}=890.41 kWh/day is the average daily yield,
- $P_{july} = 660.00\ kWh/day\ is\ the\ July\ worst - case\ yield,$
- $A = P_{mean} - P_{july} = 230.41\ kWh/day$ is the seasonal amplitude,
- t is the day index,
- t_0 is the phase shift used to align the minimum output with July.

This formulation reproduces the expected annual rise and fall in solar availability with the rainy season corresponding to lower production and the dry season to higher production.

2.12.2 Stochastic Weather Variation

To account for short-term daily irradiance uncertainty, a stochastic perturbation term was added to the seasonal profile. The final daily output was expressed as:

$$P(t) = P_{\{season\}}(t)(1-d)^{t_y} + \varepsilon_t \quad (18)$$

where:

- $d = 0.005$ *is the annual PV degradation rate,*
- t_y *is time in years,*
- $\varepsilon_t \sim N(0, \sigma^2)$ *is the Gaussian weather noise term,*
- σ *is the standard deviation of daily cloud − induced variation.*

In the MATLAB implementation, the stochastic term was generated using a normal random function which gives the model a probabilistic character while retaining the physically observed seasonal trend. In the code used for this study, σ was set to 45 kWh in the first stochastic model and 55 kWh in the extended reliability model.

2.12.3 Load Growth and PV Degradation

The village demand was allowed to increase annually to reflect appliance growth and improved electricity access. The time-dependent load was modeled as:

$$L(t) = L0(1+g)^{t_y} \quad (19)$$

where:

- $L0 = 806.20 L_0 = 806.20 L0 = 806.20$ *kWh/day is the initial village load,*
- $g = 0.02$ *is the annual load growth rate,*
- t_y *is time in years.*

The PV output degradation was modeled as:

$$D_{PV}(t) = (1-d)^{t_y} \quad (20)$$

where $d = 0.005$ *is the annual degradation rate.*

These two trends act in opposite directions on reliability: while load growth increases demand pressure, PV degradation gradually reduces available supply. The combined effect explains why reliability falls over the project life even when the system remains adequate in the early years.

2.12.4 Reliability Indices and Energy Adequacy

System adequacy was evaluated by comparing daily generation with the corresponding daily demand. The annual reliability index was computed as:

$$R_y = \frac{\sum_{i=1}^{N_y} 1(p_i \geq L_i)}{N_y} \times 100 \quad (21)$$

where:

- R_y *is the reliability in year* y,
- N_y *is the number of days in year* y,
- $I(\cdot)$ *is the indicator function,*
- P_i *is the simulated daily PV output,*
- L_i *is the daily load demand.*

The annual Loss of Power Supply Probability (LPSP) was calculated as:

$$LPSP_y = \frac{ENS_y}{\sum_{i=1}^{N_y} L_i} \quad (22)$$

where ENS_y is the annual Energy Not Served:

$$ENS_y = \sum_{i=1}^{N_y} L_i \max(0, L_i - P_i) \quad (23)$$

These metrics quantify not only whether the system meets demand, but also the magnitude of unmet load whenever generation falls short.

2.12.4.1 Time-Step Selection and Model Limitations

A daily time step was selected because the field survey produced daily appliance-energy estimates and because the principal objective was to examine seasonal adequacy, battery energy balance, and 25-year degradation at manageable computational cost. Daily chronological simulation preserves the sequence of surplus and deficit days and is therefore more informative than an annual energy balance. Nevertheless, it cannot resolve sub-hourly cloud transients, motor-starting currents, feeder voltage deviations, or short-duration inverter overloads. Peak inverter and conductor ratings were therefore sized independently using coincident demand and engineering margins. The reported LPSP and reliability indices should be interpreted as energy-adequacy indicators, not as substitutes for an hourly power-quality or protection-coordination study. A future detailed design should use measured 15-minute or hourly demand and irradiance data.

2.12.5 Battery State-of-Charge and Capacity Fade

Battery performance was modeled using daily state-of-charge tracking and capacity fade. The net daily energy balance was expressed as:

$$E_{bal,i}i = P_i\eta_{ch} - L_i \quad (24)$$

where η_{ch}=0.90 is the charging efficiency.

The battery SoC update was enforced within allowable bounds:

$$S_oC_i = \min\left(S_oC_{max}\, max\left(S_oC_{min}\, S_oC_{i-1}\frac{E_{bal,i}}{E_{bat,i}}\right)\right) \quad (25)$$

where:

- $SS_oC_{min} = 0.30$
- $S_oC_{max} = 1.00$
- $E_{bat,i}$ *is the available battery capacity in year iii.*

Battery aging was represented as the combined effect of calendar and cycling degradation rather than as an invariant annual loss. The annual capacity change was written conceptually as $\Delta C_y = \Delta C_{cal}(T_y, SoC_y) + \Delta C_{cyc}(EFC_y, DoD_y, C-rate_y)$, where EFC is the number of equivalent full cycles. The temperature and cycling correction factors increase capacity loss when the battery operates at elevated temperature, high average state of charge, high depth of discharge, or high charge/discharge rate. Because chemistry-specific aging coefficients for the selected commercial battery were unavailable, the lifecycle model was implemented as a bounded scenario envelope: 1.5%/year (managed operation), 3.0%/year (base case), and 5.0%/year (severe thermal/cycling stress). Replacement is triggered when usable capacity approaches 80% of initial capacity or when safety diagnostics require earlier intervention.

$$E_{bat}, i = E_{bat,0}\,(1-f)^i \quad (26)$$

where $f = 0.03$ is the annual battery fade factor used in the lifecycle reliability model.

The 3% value is therefore retained only as the central scenario, not as a universal physical constant. This treatment is consistent with evidence that lithium-ion aging depends on temperature, depth of discharge, state-of-charge window, and cycling intensity (Luo et al., 2023). The scenario envelope prevents the analysis from implying false precision while showing how storage aging, PV degradation, and demand growth interact. The model also assumes active battery management, restricted depth of discharge, thermal monitoring, and replacement of degraded modules or racks rather than compulsory simultaneous replacement of every unit.

For interpretation of the degradation envelope, the remaining capacity after ten years is approximately 86.0% for the 1.5%/year case, 73.7% for the 3.0%/year case, and 59.9% for the 5.0%/year case before any condition-based replacement. The Years 10 and 20 replacement entries used in the economic cash flow are therefore budget placeholders rather than fixed physical failure dates. In operation, individual modules or racks should be replaced when measured state of health, internal resistance, temperature behavior, or safety diagnostics exceed the manufacturer's limits.

2.12.6 Response Surface Methodology for Environmental Sensitivity

To examine the effect of irradiance and temperature on PV output, Response Surface Methodology was applied using irradiance (G) and temperature (T) as the independent variables. The output power surface was expressed as:

$$P(G,T) = \frac{G.A.\eta}{1000}\ [1 + \beta(T - 25) \quad (27)$$

where:

- $A = 866.16m^2$ *is the array area,*
- $\eta = 0.20$*is the module efficiency,*
- $\beta = -0.0038\beta K_1$ *is the temperature coefficient,*
- 25℃ *is the standard test condition temperature.*

This sensitivity analysis demonstrates that higher irradiance increases output, while higher temperature reduces it due to the negative temperature coefficient of the modules.

2.12.7 Technical Uncertainty and Sensitivity Analysis

Robustness was evaluated using two complementary procedures. First, stochastic daily PV output was generated by superimposing random irradiance perturbations on the seasonal resource profile, while the 2% and 5% annual load-growth cases represented alternative demand trajectories. Second, a transparent one-at-a-time and combined sensitivity screen varied commissioning-year mean irradiance and load by ±10%. The screening metric was the average daily energy margin, $M = E_{P_v} - E_L$, and the adequacy ratio, AER = $E_{PV}\ /E_L$. These scenarios do not replace the chronological battery simulation; they identify which assumptions most strongly influence the reserve margin and whether the deterministic design remains robust when average conditions shift.

The adverse combined case applies a 10% irradiance reduction and a 10% load increase, representing a cloudy year coincident with under-estimated demand. Seasonal extremes are assessed separately using the observed July minimum and dry-season maximum. Interannual variability is discussed as a planning risk because consecutive low-resource years can prevent full battery recovery even when the long-term average energy balance is positive.

2.13 Battery sizing optimization

The battery bank was optimized through an exhaustive discrete cost–reliability search rather than treated only as a fixed autonomy-based component. The primary decision variable was the autonomy duration A, evaluated from 1.0 to 5.0 days in 0.25-day increments, with the corresponding integer number of battery units N_b obtained from the usable-energy requirement. The objective function was min $C_b = N_b\ c_b$, where c_b is the unit battery cost. Feasibility constraints were Reliability ≥ 95%, LPSP ≤ 0.05, minimum allowable SoC ≥ 30%, and integer equipment quantities. For each candidate, nominal and usable storage, number of series–parallel units, battery cost, energy not served, LPSP, and reliability were computed using the same chronological energy-balance model.

Because every candidate in the finite search space was evaluated, convergence was achieved when the final autonomy candidate had been tested and the least-cost feasible solution remained unchanged; no gradient tolerance or stochastic optimizer stopping rule was required. The procedure is reproducible from the stated equations, candidate interval, reliability constraints, and component price. The selected configuration is the lowest-cost candidate satisfying all constraints, while the original three-day design is retained as a

conservative upper-bound option for sites that prioritize additional resilience over minimum cost.

3. Results and Discussion

3.1 Field-Survey-Based Daily Electrical Load Profile of Itunta Village

Table 1 presents the appliance types, quantities, rated power, and average daily operating hours recorded for households, community facilities, and small commercial activities in the study area.

Table 1: Appliances Load Chart – Itunta Village (approximate of 136 Households)

S/N	Appliance	Power (W)	Quantity	Total Power (W)	Hours/Day	Daily Energy (Wh)
1	LED Bulbs (Indoor/Outdoor)	20	500	10,000	12	120,000
2	Ceiling/Table Fans	60	150	9,000	10	90,000
3	Refrigerators (household)	200	80	16,000	10	160,000
4	Deep Freezers (shared use)	500	10	5,000	10	50,000
5	Televisions	100	100	10,000	6	60,000
6	Satellite TV Decoders (GoTV, etc.)	6	100	600	6	3,600
7	Electric Irons	1000	30	30,000	1.5	45,000
8	Sumo Water Pumps (shared)	1000	10	10,000	3	30,000
9	LED Flood Lights (security)	30	80	2,400	10	24,000
10	Desktop/Laptop Computers	70	50	3,500	4	14,000
11	Mobile Phone Chargers	5	300	1,500	4	6,000
12	Modem/Wi-Fi Routers (shared)	10	20	200	12	2,400
13	Disk Players (DVD/VCD)	60	20	1,200	4	4,800
14	Electric Heaters (Portable)	600	15	9,000	1	9,000
15	PA System (Mic + Speakers)	200	5	1,000	3	3,000
16	Musical Instruments (Keyboard/Guitar)	100	10	1,000	3	3,000
17	Amplifiers	300	5	1,500	3	4,500
18	Abacha Shredding	2300	1	2,300	3	6,900

S/N	Appliance	Power (W)	Quantity	Total Power (W)	Hours/Day	Daily Energy (Wh)
	Machine					
19	Air Conditioners (health/admin use)	3000	3	9,000	8	72,000
20	Electric Motor (Grinding Machine)	745	2	1,490	4	5,960
Total Energy Consumption				806,160 Wh/day (≈ 806.2 kWh/day)		

3.2 Secondary data collection

The meteorological data presented in Figure 3 and Tables 2–3 were obtained from PVGIS for the study location. Technical specifications and price inputs were obtained from manufacturer datasheets and documented market sources. Figure 4 presents the MATLAB-generated mounting-plane model used to illustrate panel orientation and tilt.

Table 2: PV off grid parameters for Itunta village

Parameter	Value
Latitude (decimal degrees)	5.433
Longitude (decimal degrees)	7.633
Radiation Database	PVGIS-SARAH3
Slope of PV Modules (degrees)	35
Azimuth of PV Modules (degrees)	0
Simulation Duration (Days)	6,939

Table 3: Monthly Average Solar Irradiance and Temperature Data (2005-2022)

month	*year*[1]	*H(h)_m*	*H(i_opt)_m*	*H(i)_m*	*Hb(n)_m*	*Kd*	*T2m*
Jan	2013.5	182.04	194.79	196.65	157.58	0.41	28.07
Feb	2013.5	168.34	174.99	175.8	127.28	0.45	28.42
Mar	2013.5	170.6	171.44	171.26	100.8	0.55	27.5
Apr	2013.5	164.28	160.34	159.3	109.06	0.5	26.81
May	2013.5	154.6	147.28	145.67	104.73	0.51	25.92
Jun	2013.5	135.08	127.76	126.19	84.77	0.56	24.85
Jul	2013.5	124.48	119.02	117.82	66.6	0.63	24.34
Aug	2013.5	130.76	127.11	126.22	66.63	0.63	24.39
Sep	2013.5	132.99	132.2	131.8	73.9	0.6	24.55
Oct	2013.5	153.45	156.95	157.26	101.46	0.52	25.01
Nov	2013.5	161.58	170.73	172.01	126.96	0.45	26.06

[1] The year column now shows 2013.5 as a placeholder to indicate that these are averages across all years from the 2005 to 2022.

Dec	2013.5	178.91	192.93	195.02	158.01	0.41	27.24

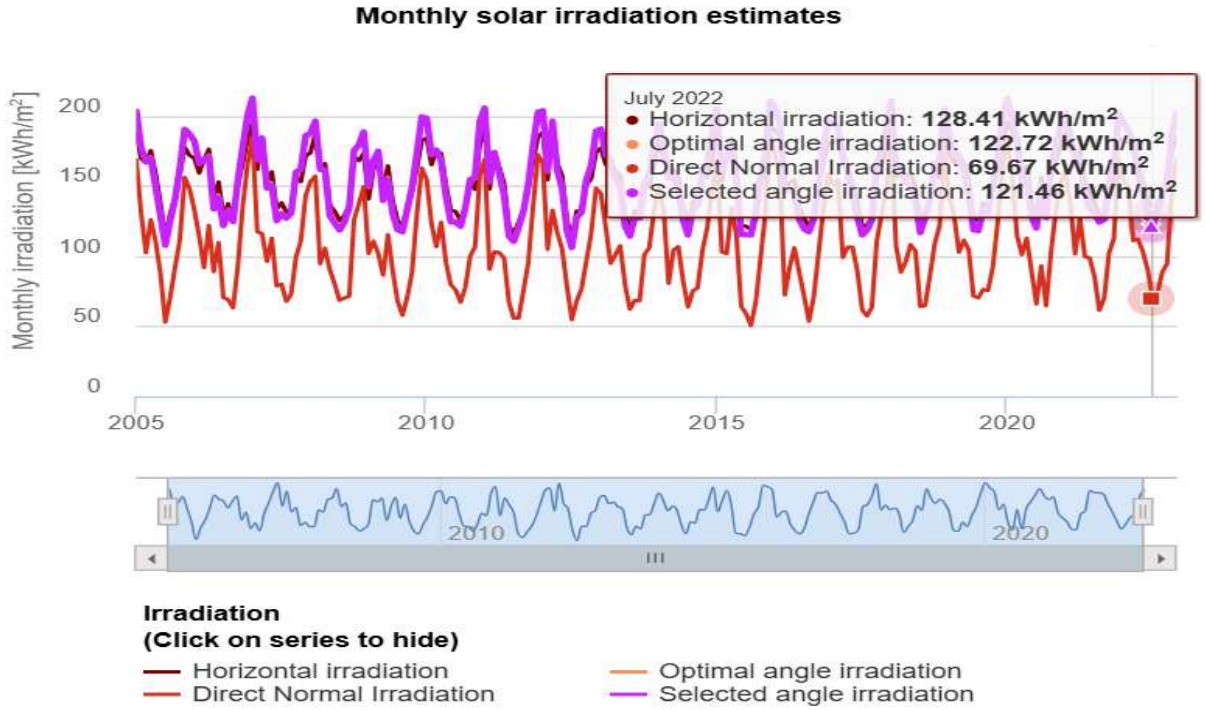

Figure 3: Monthly Solar irradiation estimates

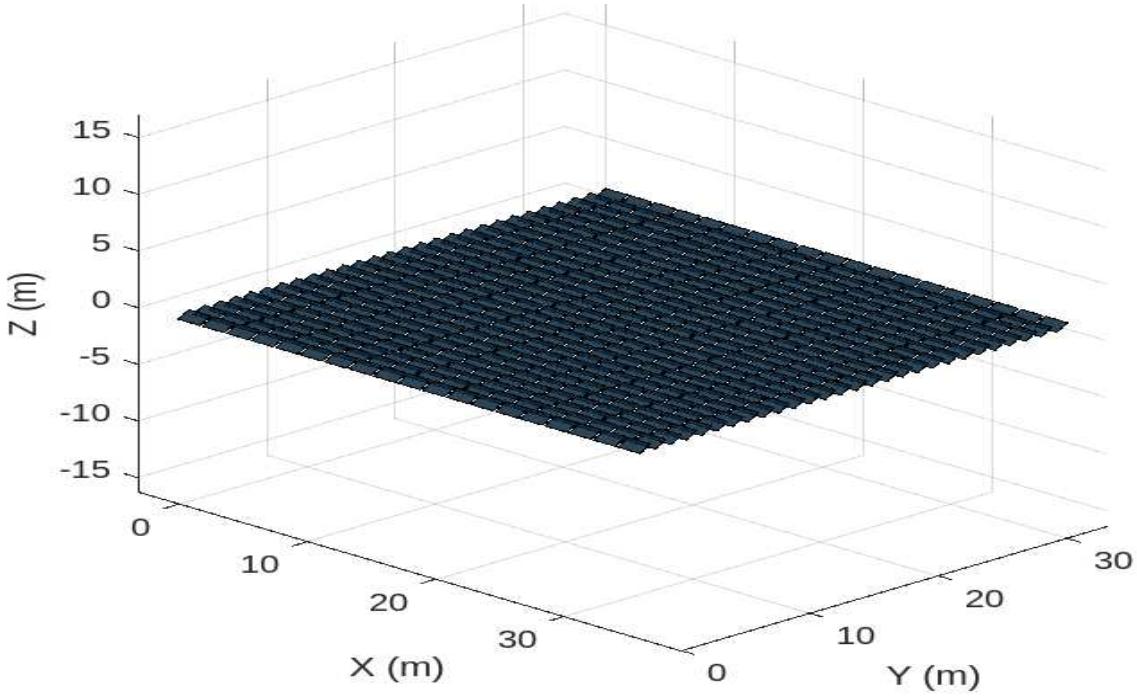

Figure 4: 3D model of Solar panel mounting structure showing the orientation and tilt

3.3 Solar Panel Technical Specification

Table 4 summarizes the technical specifications of the selected SunPower 435 W module and the principal assumptions for the balance-of-system components. The 20% module efficiency reduces the required active area. Nominal operating cell temperature and the power-temperature coefficient were taken from the manufacturer datasheet, while inverter, controller, battery, loss, depth-of-discharge, and autonomy assumptions are stated explicitly to support reproducibility.

Table 4: Characteristics of the selected SPV system components

Parameter	Value	Unit	Manufacturer/Model
Solar Photovoltaic Panel Capacity	435	W	SunPower SPR-435NE-WHT-D
Type	E 20/435 Solar Panel		SunPower
Efficiency (ηr)	20	%	SunPower
Nominal Operating Cell Temperature (NOCT)	45	°C	SunPower
Temperature Coefficient (βp)	-0.38	%/K	SunPower
Solar Collector Area (Sp)	2.16	m²	SunPower
Battery Capacity (Single)	250	Ah	Lithium-ion
System Voltage (DC)	24	V	Designed
Inverter Efficiency (ηi)	96	%	Assumed
Charge Controller Efficiency (ηc)	95	%	Assumed
Battery Efficiency (ηb)	90	%	Assumed
Depth of Discharge	0.5		Assumed
Battery Days of Autonomy	3	Days	Assumed
Energy Loss in System (ELS)	1.3	Factor	Assumed
Panel Generation Factor (PGF)	3.596		Derived for Nigeria

3.4 Technical Design and Performance Analysis of the Itunta Village Solar PV System

The technical sizing of the Itunta Village solar photovoltaic system was carried out using the field-based load demand, long-term solar resource data and the component efficiencies outlined in Table 4. The installed capacity of 174.32 kWp represented by 401 modules was selected as a conservative design to ensure reliable performance under seasonal variability. This sizing approach was deterministic and reliability-driven rather than the outcome of an optimization algorithm thereby prioritizing energy security over cost minimization. The system produces an average daily energy yield of approximately 890.41 kWh/day which exceeds the estimated village demand of 806.16 kWh/day. This margin is intentional and serves as a buffer against seasonal fluctuations. The surplus energy is primarily utilized for battery charging ensuring that storage reserves are fully replenished during high solar periods. Any additional excess energy is not explicitly allocated within the present model but represents reserve capacity that can support future productive uses such as agro-processing or small-scale enterprises. The battery storage system was designed to provide three days of autonomy at a 50% depth of discharge. At the nominal 24 V subsystem level, this corresponds to approximately 5.37 MWh of installed storage and about 2.69 MWh of usable capacity. This

large storage capacity ensures system reliability during extended low-irradiance periods but also introduces significant practical considerations. These include space requirements which has been sorted out in Figure 2 which captured the vast area that can accommodate the installation. Other considerations are installation complexity, thermal management, and long-term replacement planning. The result clearly shows that storage is the dominant factor influencing both system cost and physical deployment.

A single 24 V bulk architecture would produce impractically high current and is not proposed for implementation. The 24 V value represents an individual battery module or string-building block. The village-scale plant is instead divided into modular PV sub-arrays, combiner sections, MPPT controller banks, supervised DC coupling sections, battery racks, and parallel inverter modules. Final string voltage, rack voltage, protection ratings, cable sizes, and earthing arrangements must be confirmed during detailed engineering using the selected commercial equipment. This modular interpretation reduces conductor current, isolates faults, supports staged maintenance, and permits future expansion without shutting down the entire plant.

While the numerical design results are specific to Itunta Village, the overall methodology combining field survey data, long-term solar resource analysis, deterministic sizing and reliability assessment is applicable to other rural electrification contexts with different demand and environmental conditions. See Table 5.

Table 5: Summary of System Design and Performance Results

Category	Parameter	Reference Formula	Resulting Value
Solar Array	Peak Wattage (W_p)	Eqn. (1)	174,319.2 W_p
	Total Number of Modules	Eqn. (2)	401 Panels
	Total Solar Area (SA)	$N \times Area_p$	866.16 m²
Storage	Total Battery Capacity	Eqn. (3)	223,933.3 Ah
	Total Number of Batteries	Eqn. (4)	896 Units
BoS	Charge Controller (SCC)	Eqn. (5)	3,223.04 A
	Inverter Capacity	Eqn. (6)	150,000 W
Performance	Daily Energy Yield (E)	Eqn. (7)	890.41 kWh/day
	Performance Ratio (SPR)	Eqn. (11)	90.54 %
Electrical	Max DC Current	Eqn. (8)	20,855 A
	Max AC Current	Eqn. (9)	1,518 A

3.5 Technical Analysis of Solar Resource Reliability and Load Fulfillment

The system performance over the year is evaluated through the relationship between solar energy generation and community demand. The results show a clear seasonal pattern that reflects the variability of solar resources in Nigeria. During the high-irradiance months particularly January, February, and December, energy production significantly exceeds the daily demand. This surplus is first used to charge the battery system ensuring that adequate reserves are available for periods of reduced solar input. Any remaining excess energy represents an opportunity for future demand-side expansion.. In contrast, the rainy season, especially between June and August is characterized by reduced solar output. The lowest production occurs in July where generation falls below demand. During this period, the battery

system compensates for the shortfall maintaining supply continuity. This seasonal deficit confirms the importance of storage capacity in ensuring reliable operation.

3.5.1 Solar Performance Ratio across the Months

The system's efficiency in meeting demand is further detailed in the Monthly SPR Variability as illustrated by Figure 5. The Solar Performance Ratio (SPR) acts as a metric for system stress where higher percentages indicate a greater reliance on the total available solar capacity. The system maintains a Mean SPR of 90.54% which indicates a well-balanced design that effectively converts available solar resources into useful work throughout the year.

The analysis establishes a red dashed System Limit line at 100% to mark the threshold where demand equals the maximum potential yield. During the months of June, July, August, and September, the SPR exceeds this 100% threshold peaking at 122.4% in July. These over-limit SPR values highlighted by the orange bar for July confirm that instantaneous solar yield is mathematically insufficient to meet the village load on its own during the rainy season. This numerical data proves the absolute necessity of the oversized battery storage system and the high-capacity 3,223A charge controller configuration to manage these seasonal energy shifts successfully. In summary, the integrated data from the figure confirms that while the 174.3 kWp array provides an annual surplus, the battery storage is the critical component that guarantees 24-hour reliability for the Itunta Village community. The system design is therefore validated as capable of overcoming the disparate weather patterns of Nigeria by strategically storing excess energy during the dry season to cover the predicted deficits in the rainy season.

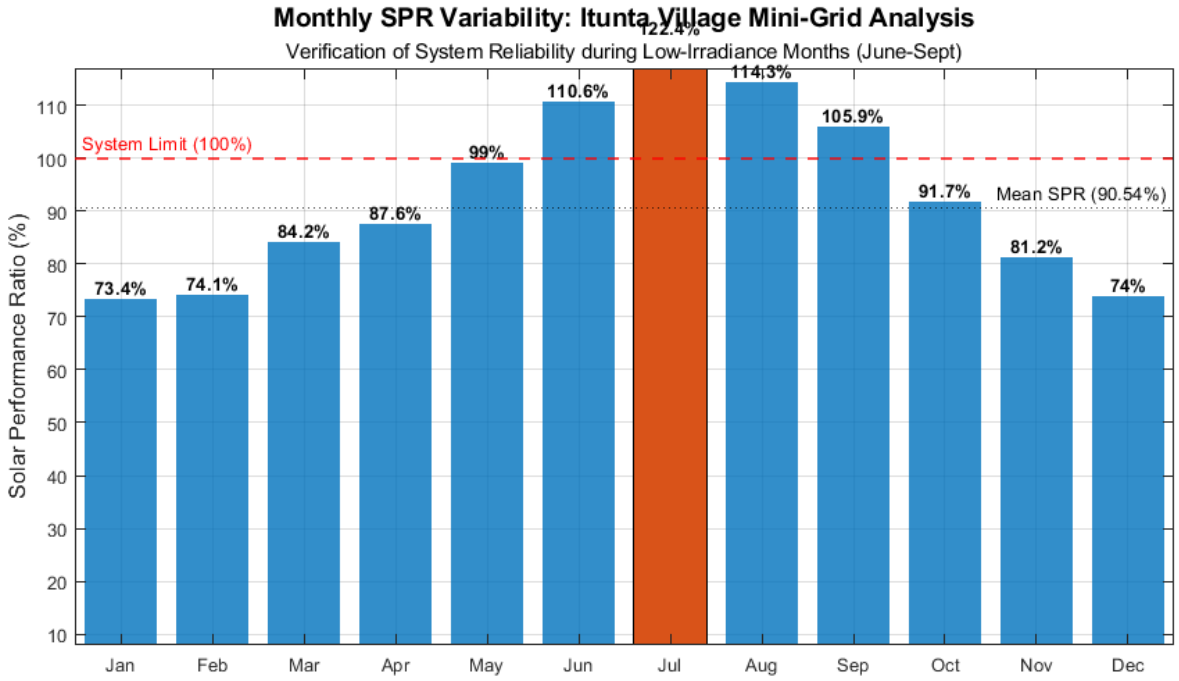

Figure 5: Solar Performance Ratio across the Months

3.6 System Configuration and Wiring Logic

To translate the calculated capacities into a physical installation, the proposed system was arranged as a modular photovoltaic and battery architecture. The design is built around PV string grouping, parallel charge-controller inputs, battery stringing, and centralized DC-to-AC conversion so that the plant can be implemented safely and efficiently.

3.6.1 Solar Array String Configuration

The 401 SunPower 435 W modules were arranged into series-parallel groups to achieve the required 174.32 kWp while keeping the current in each branch manageable. The array is therefore not treated as a single low-voltage block but as multiple PV strings feeding MPPT-based controller banks. This arrangement improves charging efficiency, reduces cable stress and supports practical power distribution within the mini-grid. The string grouping also helps the array interface properly with the battery subsystem and the inverter stage. In practice, this makes the system more suitable for field installation because the generation side is divided into smaller controllable sections rather than being concentrated in one large circuit.

3.6.2 Battery Bank Matrix Design

The conservative three-day storage case consists of 896 lithium-ion units of 250 Ah each, while the optimized one-day case uses 598 units. In either case, the units are grouped into manufacturer-approved racks and strings, each with rack-level battery management, isolation, fusing, temperature sensing, and accessible maintenance clearances. The storage enclosure requires restricted access, ventilation or active cooling, fire detection, emergency isolation, spill-free drainage design, and separation from occupied buildings. A phased replacement strategy is preferable to simultaneous replacement: modules are screened by state of health, weak racks are replaced first, and reusable units are retained where safe and electrically compatible. See Table 6, Figure 6, and Table 7.

Table 6: Summary of Connection Specifications

Component	Total Units	Configuration Logic	Resulting Parameter
Solar Modules	401 Panels	Series-parallel string groups feeding MPPT banks	174,319.2 Wp
Battery Units	896 conservative / 598 optimized	Manufacturer-approved modular battery racks with BMS, isolation, and series–parallel grouping	3-day upper bound / 1-day recommended
Charge Controllers	Multiple Units	Parallel MPPT charge-controller banks	Distributed charging capacity
Main Inverter	150 kW System	Central DC-to-AC conversion stage	230 V AC Output

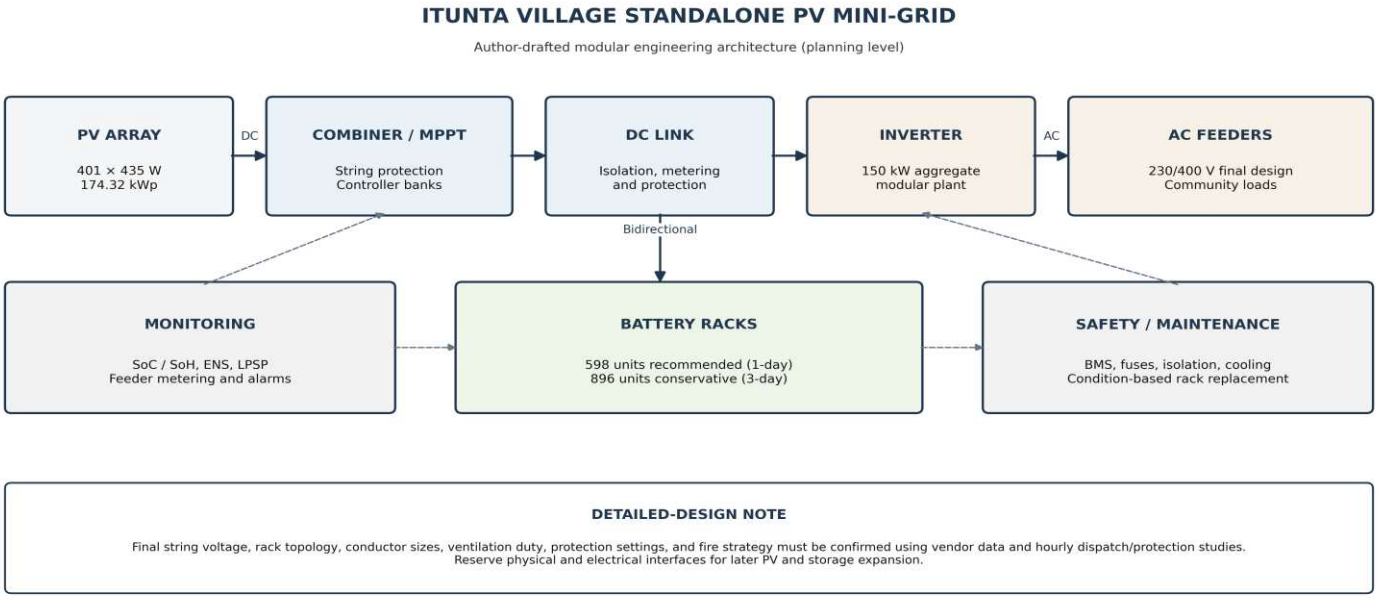

Figure 6: Author-drafted modular engineering architecture of the Itunta Village standalone PV mini-grid

Practical implementation, operation, and safety requirements

The calculated storage capacity has major practical implications. Implementation should be divided into independently isolatable battery and PV blocks so that inspection or replacement of one block does not interrupt the whole community. A local operator should maintain daily alarm and meter records, while trained technicians perform periodic torque checks, insulation tests, thermal scans, protection tests, and state-of-health reviews. The replacement budget must be ring-fenced from the start of operation because battery expenditure dominates the lifecycle cost. End-of-life batteries should be transferred through authorized collection and recycling channels rather than stored indefinitely at the site.

Table 7: Practical implementation, maintenance, safety, and replacement plan

Issue	Engineering requirement	Recommended management action
Installation and space	Separate PV field, inverter room, and restricted battery enclosure; provide access aisles and lifting routes.	Complete detailed layout, geotechnical check, drainage design, shading study, and staged construction plan.
Thermal management	Maintain manufacturer-specified temperature range with ventilation or active cooling and continuous temperature sensing.	Log rack temperatures; alarm on abnormal rise; derate or isolate affected racks.
Electrical and fire safety	Rack-level BMS, DC fuses/contactors, isolators, surge protection, earthing, arc-fault/overcurrent protection, and emergency shutdown.	Train operators; post single-line diagrams and emergency procedures; inspect protection devices routinely.
Maintenance	Module cleaning, vegetation control, cable/connector inspection, inverter servicing, and SoC/SoH monitoring.	Daily remote checks, monthly visual inspections, quarterly electrical checks, and annual comprehensive service.
Replacement strategy	Capacity-triggered rack replacement rather than automatic replacement of all units.	Budget for Years 10 and 20; test modules, replace weak racks first, and rebalance strings.
Operations and demand growth	Productive-use loads can exceed the original forecast and accelerate storage stress.	Use feeder metering, demand limits, tariff/load-management rules, and planned PV/storage expansion.
End of life	Battery and electronic waste require controlled collection, transport, and recycling.	Use authorized recyclers and maintain waste-transfer records.

3.7 Techno-Economic Analysis

3.7.1 System Capital Expenditure (CAPEX) Estimation

The capital expenditure (CAPEX) of the proposed mini-grid system was estimated using unit cost rates in Nigerian Naira (₦) applied to the full-scale component requirements of the village. The solar photovoltaic (PV) array consists of 401 panels priced at ₦82,000 per unit resulting in a total cost of ₦32,882,000. The battery bank which represents the dominant cost component comprises 896 units at ₦575,997 each giving a total of ₦516,093,312. The charge controller requirement was determined based on the total system current of 3,223 A divided by a 30 A controller rating yielding a cost of ₦4,931,190. Similarly, the inverter system was sized using a 150-kW demand divided into 4 kW units resulting in a total cost of ₦2,696,250. In addition, the balance of system (BoS) components and installation costs were conservatively estimated as 5% of the total component cost, amounting to ₦27,830,138. Summing all components, the total system CAPEX is estimated at ₦584,432,890 which provides a comprehensive financial basis for the techno-economic evaluation of the proposed rural electrification system.

3.7.2 Levelized Cost of Electricity (LCOE)

The Levelized Cost of Electricity (LCOE) represents the average life-cycle cost of delivering electricity from the Itunta Village mini-grid over its projected 25-year operational lifespan. The estimate incorporates the system capital expenditure, annual operation and maintenance costs, long-term energy generation and key financial assumptions governing system performance. To ensure transparency and reproducibility, the financial parameters adopted in the analysis are presented in Table 8

Table 8: Financial assumptions used for LCOE and payback analysis

Parameter	Value	Unit	Remark / Justification
Project lifetime	25	years	Standard planning horizon
Discount rate (real)	10	%	Moderate financing condition
Inflation rate	8	%	Nigerian long-term estimate
Analysis type	Real-term	–	Constant Naira basis
Annual O&M cost	1.0	% of CAPEX/year	Maintenance & operations
PV degradation rate	0.5	%/year	Manufacturer-based
Battery degradation rate	3.0	%/year	Central case; 1.5–5%/year sensitivity envelope
Battery replacement year	10 and 20	years	Cash-flow placeholders; operation is condition-based
Battery replacement cost factor	50	%	Reduced due to oversizing and partial utilization
Inverter replacement year	12	years	Typical lifespan
Inverter replacement cost factor	80	%	Includes installation
System availability	95	%	Accounts for downtime
Annual energy	325,000	kWh/year	From system simulation

production			
Total lifetime energy	8,125,000	kWh	Over 25 years
Diesel benchmark cost	450	₦/kWh	For economic comparison
Salvage value	0	₦	Conservative assumption

Base-Case LCOE Estimation (Simplified Model)

A simplified base-case LCOE was first computed using total capital cost and cumulative operation and maintenance expenditure over the project lifetime without discounting or replacement cost treatment. Using a CAPEX of ₦584,432,890, annual O&M cost of 1% of CAPEX, and total lifetime energy generation of 8,125,000 kWh, the resulting base-case LCOE is:

$$LCOE_{base} \approx ₦89.91 kWh$$

This value represents an idealized lower-bound estimate, useful primarily for benchmarking purposes. S8

Extended Life-Cycle Cost Analysis (Discounted Model)

To capture real-world economic conditions, a full life-cycle model incorporating discounting, inflation, and component replacement was implemented. Under the base financial scenario (10% discount rate, 8% inflation, and 50% battery replacement cost), the resulting LCOE is:

$$LCOE_{realistic} \approx ₦358.63 kWh$$

This substantial increase relative to the simplified estimate highlights the strong influence of financing conditions and storage reinvestment on standalone mini-grid economics. The adoption of a 50% battery replacement cost factor is justified by the system design characteristics. The battery bank is intentionally oversized to ensure reliability under worst-case solar conditions, meaning that a significant portion of the storage capacity is only utilized during deficit periods. Consequently, not all battery units undergo uniform degradation and partial replacement strategies can be implemented in practice. Furthermore, expected reductions in lithium-ion battery prices over time support the assumption of reduced future replacement cost.

Sensitivity Analysis

To evaluate the robustness of the economic results, a sensitivity analysis was conducted by varying key parameters which includes discount rate, inflation and battery replacement cost factor. The results are presented in Table 9. The sensitivity analysis reveals that the LCOE is strongly influenced by both macroeconomic conditions and battery system cost. Under favorable financing conditions, the LCOE reduces to approximately ₦291/kWh while adverse conditions increase it to over ₦470/kWh. Similarly, variations in battery replacement cost significantly impact system affordability which confirms that storage remains the dominant cost component in standalone solar mini-grids. The wide variation between the simplified LCOE (₦89.91/kWh) and the discounted life-cycle estimates (₦291–₦472/kWh) demonstrates that the base-case value represents a theoretical lower bound. In addition, the extended model provides a more realistic assessment of long-term system cost.

Despite this increase, the system remains competitive when compared with diesel-based electricity generation in rural Nigeria where costs typically exceed ₦450/kWh. This confirms that the proposed solar PV mini-grid remains a viable solution for rural electrification, particularly under improving battery cost trends and favorable financing conditions. It should be noted that the diesel benchmark cost of ₦450/kWh used for comparison represents a present-day static estimate and does not incorporate inflation, fuel price escalation, or lifecycle cost adjustments. In contrast, the solar PV system LCOE was computed using a discounted cash flow framework that explicitly accounts for inflation, component replacement and long-term cost dynamics. As a result, the comparison is conservative with respect to the solar system. If similar financial treatment were applied to diesel-based generation, its effective lifecycle cost would be significantly higher. This further strengthens the economic viability of the proposed solar mini-grid.

Table 9: Sensitivity of LCOE to key economic parameters

Scenario	**Discount Rate (%)**	**Inflation (%)**	**Battery Cost Factor**	**LCOE (₦/kWh)**
Simplified (no discounting)	0	0	–	89.91
Base-case (with discounting)	10	8	0.5	358.63
Low financing scenario	8	5	0.5	291.04
High financing scenario	15	12	0.5	472.53
Low battery cost	10	8	0.3	309.21
High battery cost	10	8	0.8	432.74
PV module price −20%	10	8	0.5	356.4
PV module price +20%	10	8	0.5	360.9
Battery system price −20%	10	8	0.5	≈299
Battery system price +20%	10	8	0.5	≈418

3.7.2.1 Net Present Cost, Lifecycle Cost, and Replacement Burden

Net present cost (NPC) was calculated as the present value of initial CAPEX, annual O&M expenditure, battery replacement, and inverter replacement over 25 years, less any salvage value. Using the same discounted cash-flow stream that produced the reported lifecycle LCOE, the base-case NPC is approximately ₦1.02 billion. The corresponding undiscounted nominal lifecycle cash requirement is approximately ₦2.65 billion when escalating O&M and replacement expenditures are included. These values are substantially higher than the initial ₦584.43 million CAPEX and demonstrate why initial cost alone is insufficient for investment appraisal.

Battery procurement and replacement constitute the dominant cost exposure. The component-price sensitivity results show that a ±20% change in PV module price has only a small effect on LCOE, whereas a ±20% change in battery-system price changes LCOE by roughly ±₦60/kWh. This result supports phased procurement, competitive battery tendering, strict thermal and depth-of-discharge management, and establishment of a replacement reserve fund.

3.7.3 Diesel Benchmark Cost Justification

To provide a realistic basis for economic comparison, the diesel electricity benchmark adopted in this study (₦450/kWh) was derived from a bottom-up cost model representing typical small-scale community generation in rural Nigeria. The benchmark incorporates three principal cost components: capital recovery of the generator system, fuel consumption and routine operation and maintenance (O&M) expenses. A representative 30 kVA diesel generator system including installation, wiring and auxiliary components was assumed to have a total installed cost of approximately ₦3,000,000. This cost was annualized over an estimated lifetime energy output of 112,500 kWh that yields a capital contribution of ₦26.67/kWh. Fuel cost constitutes the dominant component of diesel generation. At an average consumption rate of 0.233 L/kWh (corresponding to approximately 3.5 L/h at 50% loading) and a prevailing diesel price of ₦1,756.25/L, the fuel cost is estimated at ₦409.79/kWh. An additional allowance of ₦13.50/kWh was included to account for routine servicing, lubricants, filter replacement and minor repairs. Summing these components results in a total diesel generation cost of approximately ₦449.96/kWh which is conservatively rounded to ₦450/kWh for use as the benchmark value in this study. This value reflects real operating conditions for decentralized diesel-based electricity supply and provides a consistent basis for evaluating the economic competitiveness of the proposed solar PV–battery system.

3.7.4 Payback Period

The financial viability of the investment is further assessed through the payback period which measures the time required for the project to recover its initial investment through energy cost savings. In the Nigerian context, this is calculated by comparing the solar system's CAPEX against the high cost of diesel generation which currently averages approximately ₦450 per kWh for small-scale generators. With an annual generation of 325,000 kWh, the system achieves gross annual savings of ₦146,250,000. After deducting the annual OPEX of ₦5,844,328, the net annual savings amount to ₦140,405,672. Dividing the total CAPEX of ₦584,432,890 by these net savings results in a payback period of approximately 4.16 years indicating a highly favorable return on investment for the community. Figure 7 illustrates the project payback analysis and LCOE sensitivity analysis.

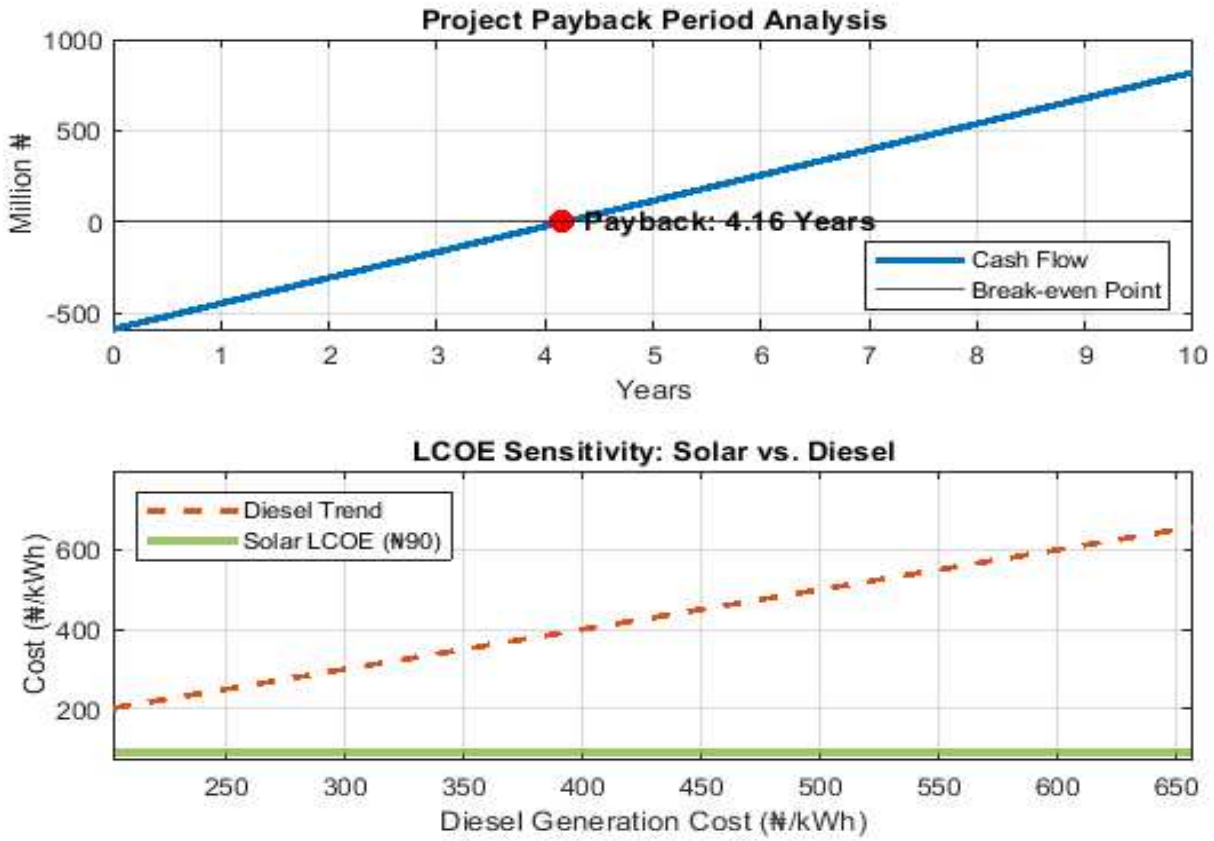

Figure 7: LCOE and project payback analysis

3.7.5 Scenario Testing: Best-Case vs. Worst-Case

Scenario testing is conducted to verify system reliability across disparate seasonal weather patterns in Nigeria. In the best-case scenario occurring during the dry season months of January and December. The daily yield exceeds 1,100 kWh/day while the Solar Performance Ratio (SPR) stays near 73.4%. This provides a massive energy surplus for battery bank recovery. Conversely, the worst-case scenario occurs in July when the daily yield drops to its lowest point of 660 kWh/day. During this period, the SPR rises to 122.4% which indicates that the village load is 22.4% higher than what the daily solar resource can provide. During this month, the system maintains reliability by relying entirely on its 3 days of autonomy and the robust 2S448P battery configuration to prevent power outages.

3.7.6 Sensitivity Analysis (Energy Payback Time - EPBT)

A sensitivity analysis focusing on the Energy Payback Time (EPBT) highlights the environmental and technical efficiency of the chosen SunPower 435W modules. The high efficiency of 20% is a critical factor that minimizes the physical footprint of the array to a total solar area of 866.16 m^2. In high-irradiation zones such as Itunta Village which experiences an average of 5.14 peak sunshine hours (PSH). The energy required to manufacture and install the panels is paid back by the system's own generation in approximately 1.3 years. This rapid energy return underscores the sustainability of the monocrystalline technology utilized in the design.

3.7.7 Technical Configuration for Connection

The final technical architecture uses modular series-parallel stringing for the PV array and battery bank with MPPT-based charge-control regulation and centralized DC-to-AC inversion. This arrangement allows the system to operate as a scalable mini-grid with manageable current paths and reduced thermal stress. The inverter system is sized to accommodate the village peak demand and to provide stable 230 V AC output for households and community facilities. Overall, the configuration reflects a practical implementation strategy for a standalone rural solar mini-grid.

3.7.8 Practical Sustainability, Environmental Management and End-of-Life Responsibility

The long-term sustainability of the proposed Itunta Village mini-grid extends beyond techno-economic performance to include land use optimization, environmental protection and end-of-life system management. The effective module area of 866.16 m² represents the active photovoltaic surface. However, the actual land requirement is higher due to inter-row spacing, tilt optimization and access pathways required to mitigate inter-array shading and facilitate maintenance operations. From an operational standpoint, the system requires structured preventive maintenance which includes periodic cleaning of modules to reduce soiling losses, thermal and electrical inspection of cables and protection systems, inverter performance monitoring and continuous assessment of battery state-of-health. The battery subsystem being the most capital-intensive and degradation-prone component demands particular attention to thermal management and controlled depth-of-discharge operation to ensure longevity.

At the end of its service life, the lithium-ion battery bank must be handled in accordance with environmental safety standards to prevent soil and groundwater contamination. In the context of Abia State, Nigeria, such responsibility falls under the regulatory oversight of the Abia State Environmental Protection Agency which is mandated to manage waste control, environmental compliance and approve disposal practices. In addition, national-level guidance from the National Environmental Standards and Regulations Enforcement Agency provides the regulatory framework for hazardous waste handling including electronic and battery waste streams. The integration of these institutional frameworks ensures that battery decommissioning, collection and recycling are conducted through authorized channels. This promotes circular resource use and minimizing environmental risk.

Overall, the sustainability of the proposed mini-grid is contingent upon coordinated land-use planning, shading mitigation, structured maintenance protocols and compliance with state and national environmental regulations governing battery disposal and recycling. These considerations ensure that the system remains not only technically viable and economically competitive but also environmentally responsible throughout its lifecycle.

3.8 Analysis of Mini-Grid Functional Longevity and Reliability

The longitudinal performance data of the Itunta Village mini-grid emphasizes the complex interplay between hardware degradation and socio-economic evolution. As evidenced by the 25-year system longevity summarized in Table 10. The system begins with an Average Daily Yield of 887.17 kWh/day in Project Year 1, providing a healthy margin over the initial demand. However, the simulation captures a critical reliability scissors effect. The

photovoltaic supply decays at a rate of 0.5% per annum and the community's energy requirement expands by 2% annually due to appliance creep and improved economic standards.

By the mid-point of the project lifecycle, the Reliability Index of the worst-case scenarios shows a marked decline, shifting from an initial 62.19% to consistently below 50% in the final years. The Days of Deficit column is particularly telling for infrastructure planning, it quantifies the increasing stress on the battery storage system. This bridges a gap that grows from 138 days in Year 1 to nearly 200 days by Year 25. It identifies a "Load Saturation Point" where the original system architecture no longer meets the village's growth trajectory which necessitates a planned capacity expansion or "energy roadmap" intervention by the second decade of operation.

Table 10: Twenty-five-year system longevity summary

Project Year	Avg Daily Yield (kWh)	Min Daily Yield (kWh)	Reliability Index of worst days (%)	Days of Deficit	Total Days
1	887.17	540.69	62.19	138	365
2	883.22	574.02	60.55	144	365
3	878.37	512.39	59.73	147	365
4	879.08	564.67	60.66	144	365
5	868.53	555.91	60.27	145	365
6	869.91	512.13	59.45	148	365
7	861.34	527.65	58.90	150	365
8	860.35	509.57	58.20	153	365
9	854.11	532.07	56.99	157	365
10	851.26	560.22	54.80	165	365
11	844.68	519.41	54.52	166	365
12	839.40	534.81	55.19	164	365
13	839.75	515.11	53.70	169	365
14	834.07	514.64	53.97	168	365
15	824.94	536.33	53.70	169	365
16	820.80	511.43	51.37	178	365
17	818.19	529.76	51.78	176	365
18	817.24	520.76	51.23	178	365
19	809.96	495.97	50.69	180	365
20	805.75	495.50	50.82	180	365
21	804.81	481.30	49.86	183	365
22	799.58	460.63	48.77	187	365
23	790.93	475.11	47.95	190	365
24	788.46	491.95	46.18	197	365
25	787.88	507.01	46.85	194	365

3.9 Interpretation of Daily Reliability Indices and Time-Step Limitations

The daily chronological model is appropriate for evaluating seasonal energy adequacy, battery reserve depletion, and long-term capacity planning because the available demand survey is expressed in daily appliance-energy terms. Unlike an annual balance, it preserves sequences of cloudy days and the carry-over of battery state of charge. However, daily

aggregation smooths short-duration mismatches and can overstate service continuity if evening peaks, motor starts, or brief cloud events exceed inverter or feeder capability. Consequently, the reported Reliability and LPSP values quantify energy sufficiency, not voltage quality, frequency stability, or interruption duration at sub-daily resolution.

This limitation does not invalidate the lifecycle findings, but it constrains their interpretation. The design should proceed to an hourly or 15-minute validation stage using metered demand before procurement. Such a study should include coincident peak demand, refrigerator and pump cycling, inverter overload capability, controller clipping, feeder losses, and protection coordination. The present results are therefore a planning-level adequacy assessment and a basis for detailed engineering rather than a final construction model.

3.10 Technical Analysis of the Simulation Visualizations

Figure 8 provides a multi-dimensional validation of the Itunta Village mini-grid's design, focusing on the intersection of stochastic environmental variables and deterministic load growth.

3.10.1. Dynamic Supply vs. Growing Load Demand (Top-Left Plot): This time-series visualization is the "heart" of the 25-year study. The blue shaded region represents the daily energy yield accounting for the Monte Carlo noise (weather uncertainty). The red line represents the 2% annual load growth. This plot identifies the "Reliability Crossover" in the early years. The degraded mean supply (blue line) stays safely above the load but as the panels age and the village adds more appliances and the supply-demand gap narrows. This provides clear visual evidence for when the system will require a capacity upgrade.

3.10.2. Response Surface Methodology: Power Output Sensitivity (Top-Right Plot): This 3D surface plot captures the sensitivity of the SunPower 435W modules to the harsh Nigerian climate. It maps power output against varying levels of Irradiance (G) and Temperature (T). The downward slope toward the higher temperature axis illustrates the negative temperature coefficient (-0.38%/K). This plot is crucial because it proves that simply having high solar irradiance is not enough. The extreme heat in regions like Nigeria shaves off potential peak power requiring the oversized 174.3 kWp array to compensate for these thermal losses.

3.10.3. Annual System Reliability Index (Bottom-Left Plot): This bar chart translates complex daily data into a simple "pass/fail" metric for stakeholders. The black dashed line represents the industry-standard target of 95% reliability. By plotting this across the 25-year horizon, we can see exactly in which "Project Year" the system falls below acceptable service levels. This graph serves as an investment roadmap indicating that while the initial capital expenditure (CAPEX) covers the first decade, operational adjustments are mandatory in the latter half of the project life.

3.10.4 Monte Carlo Yield Probability Distribution (Bottom-Right Plot): This histogram provides a statistical stress test of the system. By aggregating every simulated day over 25 years, it creates a probability density function (PDF). The area of the curve to the left of the red dashed "Initial Load" line represents the statistical probability of a blackout. This allows the study to move beyond average values and discuss the Value at Risk (VaR) proving that the system is resilient not just on average days but also during rare, high-cloud-cover events.

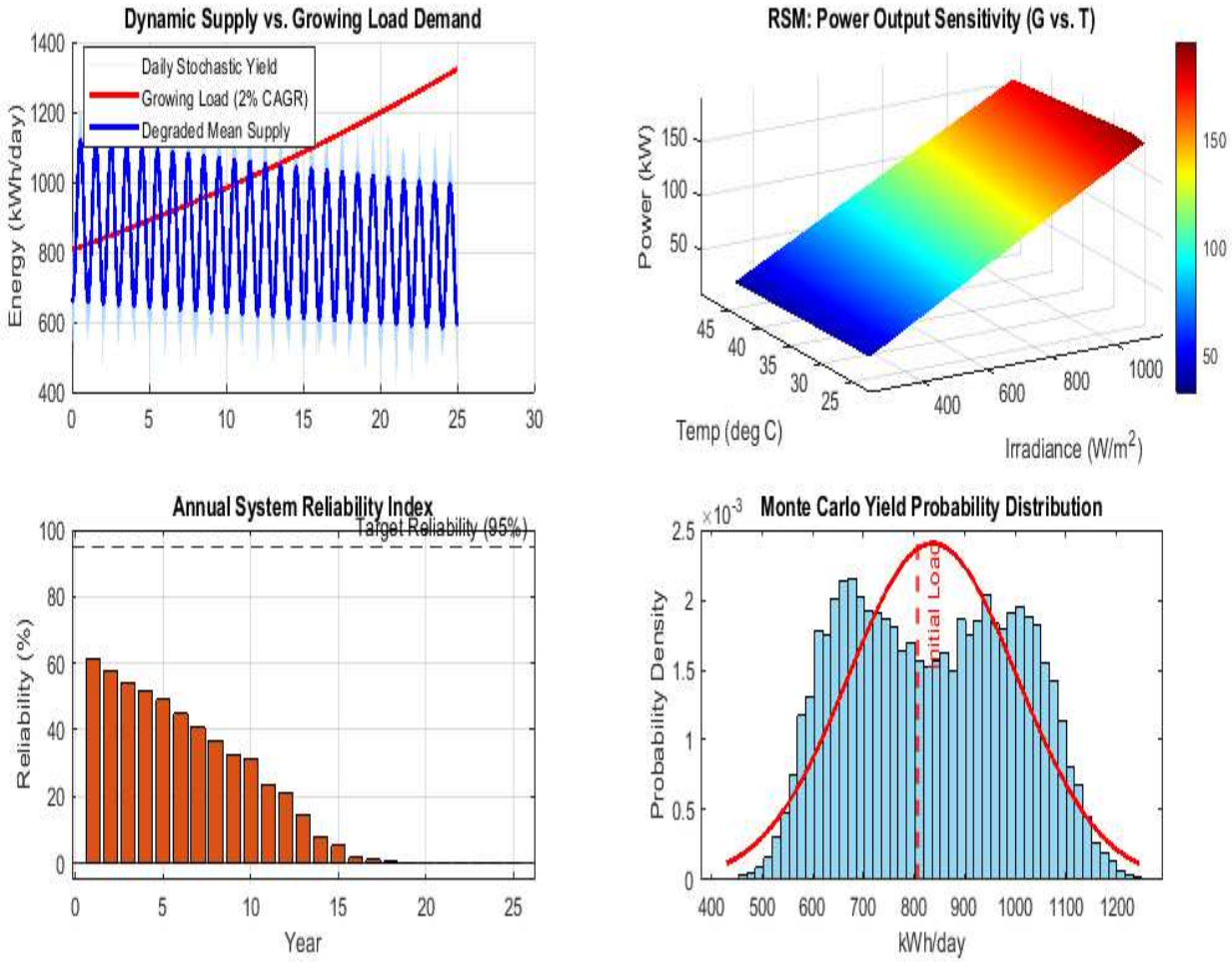

Figure 8: Multi-dimensional validation of the Itunta Village mini-grid's design

3.11 Standardized Lifecycle Reliability and Battery Performance Analysis

Table 11 provides the numerical basis for the long-term performance assessment of the Itunta Village mini-grid under both the 2% base-case annual load growth and the 5% sensitivity-case annual load growth. These results are visualized in Figure 9 where subplot (a) shows the yearly Loss of Power Supply Probability (LPSP) and subplot (b) presents the daily battery state-of-charge (SoC) dynamics for Project Year 5. Subplot (c) illustrates battery capacity fade and replacement cycles while subplot (d) shows the distribution of Energy Not Served (ENS) events. Together, Table 11 and Figure 9 provide a complete picture of how reliability, storage behavior and service adequacy evolve over the 25-year project horizon. For the 2% annual load-growth case, Figure 9(a) and Table 11 show a gradual decline in reliability over time with the system transitioning from a high-performance initial state to a more stressed condition. In Project Year 1, the system achieves a reliability of 91.82% with an LPSP of 0.0818 and an average SoC of 63.58%. By Year 25, reliability reduces to 54.26%, LPSP increases to 0.4574 and the average SoC stabilizes at the minimum protected level of 30%. This indicates that the base-case system is adequate for present demand conditions, but its reserve margin steadily narrows as load growth and PV degradation accumulate. The storage subsystem absorbs seasonal deficits effectively in the early years but the growing demand progressively reduces system adequacy.

The 5% annual load-growth case in Figure 9(a) demonstrates a much steeper decline in performance. Reliability begins at 91.20% in Year 1 but falls rapidly to 26.67% by Year 25 while LPSP rises from 0.0880 to 0.7333. The corresponding ENS values in Table 11 also increase sharply confirming that faster demand expansion overwhelms the original PV-battery sizing. By comparing

the two cases in Figure 9(a) it becomes clear that higher load growth accelerates the onset of energy deficits and substantially shortens the period over which the system remains serviceable without augmentation. The SoC behavior shown in Figure 9(b) further supports this conclusion. Under the 2% scenario, the battery SoC remains above the minimum 30% threshold for a longer period and only approaches the floor in the later part of the study horizon. In contrast, the 5% scenario reaches the 30% threshold much earlier around Project Year 5 and remains constrained thereafter. This indicates that the battery bank is the component most directly stressed by accelerated demand growth. Once the lower SoC limit is reached, the system has little buffering capacity left to absorb seasonal or daily deficits which explains the rapid rise in ENS under the higher-growth scenario.

Figure 9(c) which shows battery capacity fade and replacement cycles, indicates that even with scheduled replacement events, the system becomes increasingly vulnerable as load demand grows. The replacement cycles temporarily restore storage capacity but they do not fully offset the effect of rising demand. In the 2% case, the decline is gradual and manageable for a longer period, whereas in the 5% case the same storage architecture becomes insufficient much earlier. This confirms that load growth is the dominant driver of long-term reliability decline while battery aging and PV degradation intensify the trend. The ENS distribution shown in Figure 9(d) provides additional evidence of the difference between the two load-growth cases. Under the 2% growth scenario, ENS events remain concentrated at relatively lower deficit levels indicating that shortages occur but are still partially manageable through storage dispatch. Under the 5% scenario, the ENS distribution shifts toward much larger deficit values showing that the system experiences more frequent and more severe energy shortfalls. This confirms that faster rural electrification, productive-use expansion or small-scale industrial growth would require earlier system reinforcement through additional PV capacity, greater storage, or hybridization.

Overall, the results in Table 11 and Figure 9 show that the proposed system is technically adequate for the 2% base-growth assumption but it is not sufficient for prolonged operation under 5% annual load growth without expansion. The analysis therefore demonstrates that the 2% base growth design is appropriate for current demand conditions while future productive-use growth will require planned augmentation of the PV array, battery bank or hybrid support to preserve acceptable reliability. However, the periodic "resets" in capacity at Year 10 and Year 20 represent necessary capital reinvestments in battery hardware. Yet even with these replacements, the growing load demand eventually forces the system into a permanent state of energy deficit suggesting that a secondary generation source or significant array expansion is required by the second decade to maintain utility-grade reliability.

Seasonal and interannual resource variability add a second planning risk. The July output of approximately 660 kWh/day is below the baseline demand, so the battery must enter the rainy season at a high state of charge. Consecutive unusually cloudy months or back-to-back low-resource years would reduce the opportunity for full recovery and accelerate deep cycling. Conversely, dry-season surpluses should be directed to controlled productive uses only after reserve requirements are met. These findings support annual review of the energy margin and a reinforcement trigger based on declining minimum SoC, increasing ENS, or sustained AER below unity.

Table 11: Standardized 25-year reliability and energy-service report for the Itunta mini-grid under 2% and 5% annual load growth

Year	ENS (kWh/year) 2%	LPSP 2%	Reliability 2% (%)	Avg. SoC 2%	ENS (kWh/year) 5%	LPSP 5%	Reliability 5% (%)	Avg. SoC 5%

				(%)				(%)
1	24,304	0.0818	91.82	63.58	26,545	0.0880	91.20	62.12
2	29,158	0.0962	90.38	61.01	37,180	0.1174	88.26	56.73
3	33,010	0.1068	89.32	57.31	47,978	0.1443	85.57	50.93
4	36,968	0.1169	88.31	54.84	61,584	0.1759	82.41	41.27
5	42,599	0.1324	86.76	54.01	80,525	0.2197	78.03	30.17
6	47,986	0.1462	85.38	50.94	99,583	0.2587	74.13	30.01
7	54,507	0.1629	83.71	45.81	122,020	0.3020	69.81	30.00
8	60,247	0.1760	82.40	44.27	142,560	0.3351	66.50	30.00
9	68,805	0.1976	80.24	33.22	166,150	0.3729	62.71	30.00
10	76,056	0.2141	78.59	30.76	188,700	0.4034	59.66	30.00
11	86,078	0.2376	76.24	30.04	215,000	0.4377	56.23	30.00
12	94,765	0.2558	74.43	30.03	241,420	0.4668	53.32	30.00
13	101,660	0.2697	73.03	30.00	266,320	0.4917	50.83	30.00
14	111,300	0.2895	71.05	30.00	295,490	0.5196	48.04	30.00
15	119,190	0.3040	69.61	30.00	324,110	0.5428	45.72	30.00
16	130,620	0.3257	67.43	30.00	358,180	0.5698	43.02	30.00
17	139,920	0.3429	65.71	30.00	390,220	0.5928	40.72	30.00
18	148,310	0.3564	64.36	30.00	423,350	0.6125	38.75	30.00
19	157,570	0.3712	62.88	30.00	458,840	0.6322	36.78	30.00
20	169,190	0.3897	61.03	30.00	499,170	0.6533	34.67	30.00
21	178,670	0.4046	59.54	30.00	537,210	0.6714	32.86	30.00
22	189,770	0.4213	57.87	30.00	579,470	0.6897	31.03	30.00
23	197,890	0.4307	56.93	30.00	620,560	0.7035	29.65	30.00
24	211,220	0.4495	55.05	30.00	670,090	0.7215	27.86	30.00
25	218,640	0.4574	54.26	30.00	713,210	0.7333	26.67	30.00

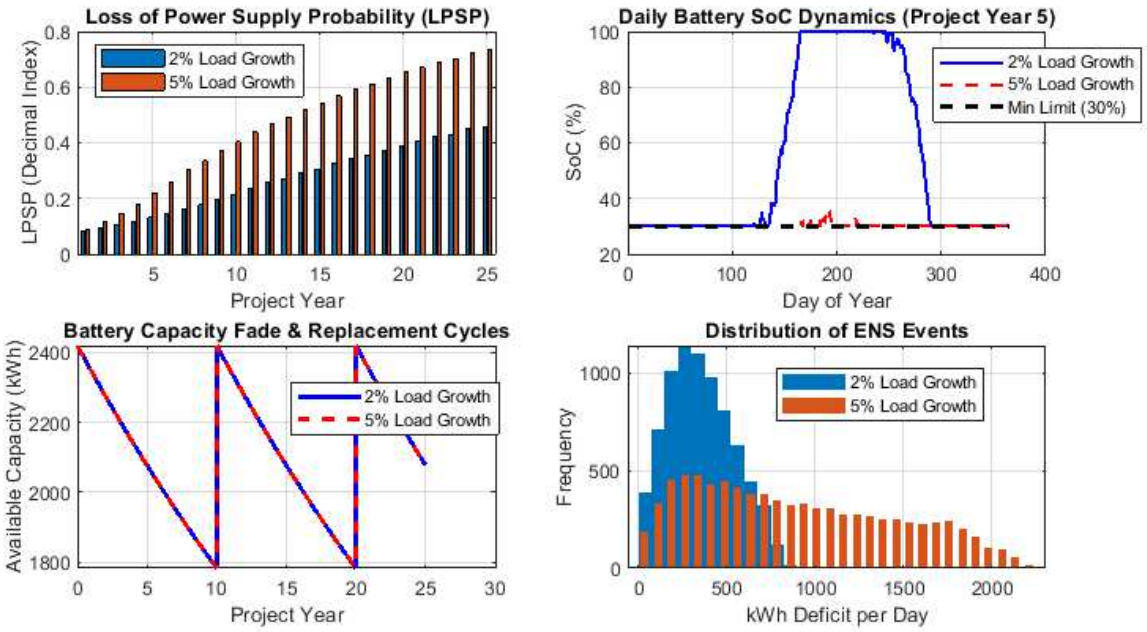

Figure 9: Longitudinal Reliability Suite including LPSP Indices, SOC Dynamics and Battery Capacity Fade Analysis (2% annual load increment)

3.12 Battery optimization outcome

Figure 10 shows that the minimum-cost feasible configuration occurs at one day of autonomy. This configuration requires 598 battery units, a nominal storage capacity of approximately 1,791.5 kWh, and usable storage of 806.16 kWh. The corresponding battery cost is approximately ₦344.45 million, with reliability of 95.974% and an LPSP of 0.040256. The original three-day design is therefore interpreted as a conservative upper-bound configuration rather than the economic optimum. The one-day case is recommended when the objective is minimum cost subject to the specified reliability constraints; the three-day case may be retained where exceptional resilience, delayed maintenance access, or prolonged extreme-weather coverage is prioritized.

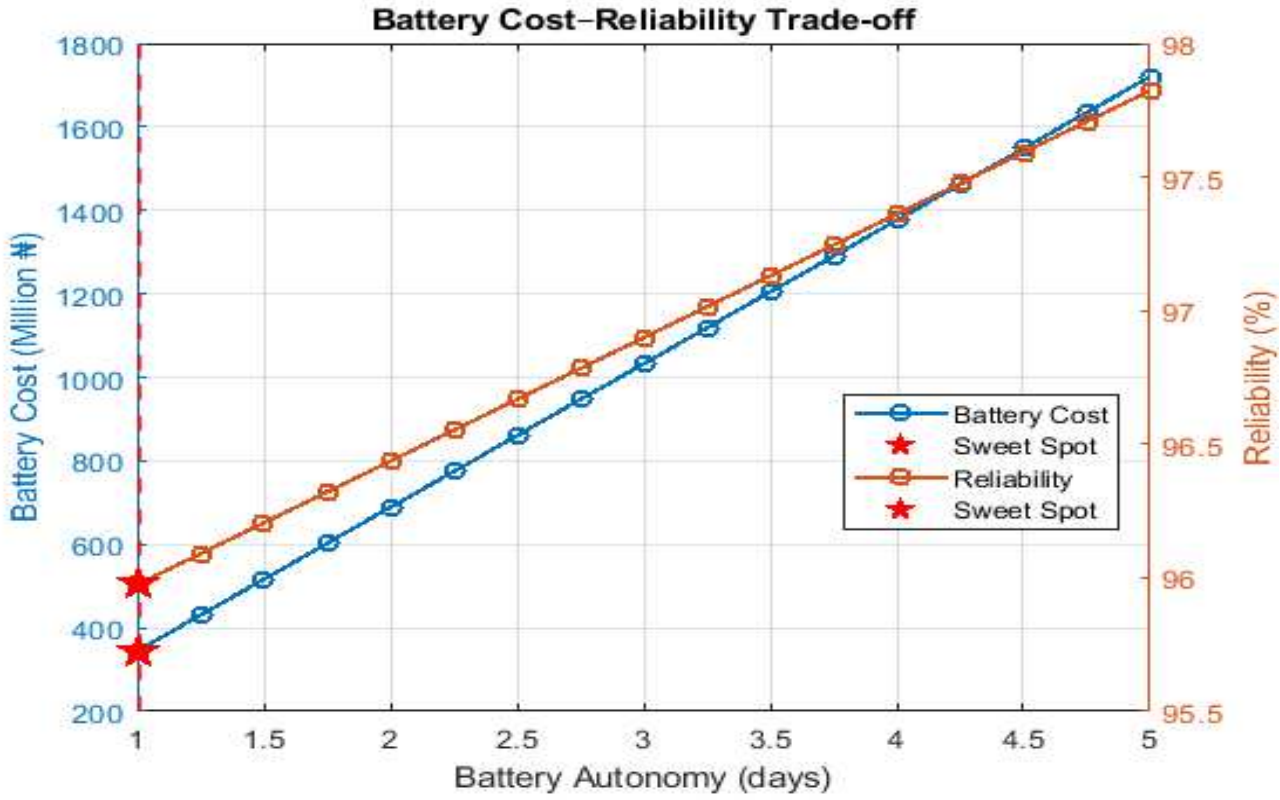

Figure 10: Battery Optimization Result

Overall, the current study confirms the main message of the literature: renewable-based microgrids are feasible and socially valuable for underserved communities. Its main contribution is that it combines field demand assessment, solar-resource validation, battery optimization, lifecycle costing and stochastic reliability analysis in one framework. Compared with previous studies, the current study is more conservative, more lifecycle-oriented and more directly applicable to rural electrification planning in environments where long-term affordability and resilience matter as much as initial feasibility.

Table 12. Commissioning-Year Technical Sensitivity to Irradiance and Load Uncertainty

Scenario	Mean PV Yield (kWh/day)	Mean Load (kWh/day)	Energy Margin (kWh/day)	Adequacy Ratio	Interpretation
Baseline	890.41	806.16	+84.25	1.104	Positive but limited reserve margin
Low irradiance (−10%)	801.37	806.16	−4.79	0.994	Average generation no longer covers demand

High load (+10%)	890.41	886.78	+3.63	1.004	Reserve margin is almost exhausted
Combined adverse	801.37	886.78	−85.41	0.904	Requires load control, additional PV, or hybrid support
Favorable (+10% PV, −10% load)	979.45	725.54	+253.91	1.350	Strong charging and productive-use potential

3.13 Technical Uncertainty and Robustness Results

Table 12 shows that the baseline average energy margin is only 84.25 kWh/day (10.4% of demand). A 10% reduction in mean irradiance changes the margin to −4.79 kWh/day, while a 10% load increase leaves only 3.63 kWh/day of average surplus. The combined adverse case produces an average deficit of 85.41 kWh/day. Storage can bridge short sequences of deficit days, but it cannot compensate indefinitely for a structurally negative mean energy balance. The result demonstrates that the design is sensitive to both resource under-performance and demand under-estimation and that the conservative or optimized storage choice must be accompanied by demand monitoring and a defined expansion trigger.

3.14 Comparative Analysis of the Present Findings with Related Research

The comparison distinguishes differences in scale, configuration, software, and performance metric rather than comparing isolated LCOE or performance-ratio values without context. Table 13 shows that grid-connected and hybrid studies generally report lower reliability risk because they can export energy or use dispatchable backup, whereas the present PV-only case carries the full storage burden. The closest Nigerian benchmark is Lewis et al. (2024), which considered a 610 kWh/day community using HOMER and obtained an optimized PV–battery–generator system. The Itunta study addresses a larger daily load and deliberately isolates the long-term behavior of a PV–battery architecture under load growth and battery aging.

The comparison also clarifies the methodological advance and its limits. Quiles-Cucarella et al. (2023) provide a more sophisticated stochastic optimization algorithm and hourly representation, but at household scale. Mohammed et al. (2022) provide extended autonomous PV/battery sizing and experimental validation, while Benchrifa and Mabrouki (2022) report strong economic performance for a grid-connected plant without storage. The present work contributes a field-surveyed village load, a 25-year load-growth and degradation trajectory, explicit storage replacement economics, and an implementation plan. It does not claim to replace commercial tools such as HOMER or PVsyst; rather, the literature benchmark provides an external plausibility check and identifies the next validation step for detailed design.

Across the literature, the general conclusions are consistent: storage size, financing assumptions, and demand growth dominate rural mini-grid viability. The Itunta results fall within the range of published community-scale studies once differences in backup generation, currency, system boundary, and discounting are recognized. A direct HOMER or PVsyst replication remains desirable before procurement, particularly to verify hourly dispatch, clipping, and loss assumptions; this requirement is now stated explicitly as a limitation and future validation activity.

Table 13. Comparison of the Present Study with Selected Related Literature

Study	Location /	Configuration and	Selected Reported	Relationship to Present Study

	Scale	Method	Result	
Mbinkar et al. (2021)	Sub-Saharan rural community	PV mini-grid design and economic assessment	Demonstrated technical feasibility of community PV mini-grids	Provides baseline sizing context; limited long-term degradation and load-growth treatment.
Benchrifa & Mabrouki (2022)	Morocco, 220 kWp establishment	Grid-connected PV simulation and economic evaluation	PR 83.1%; LCOE 0.034 USD/kWh	Lower-cost boundary without off-grid battery burden; not directly comparable to standalone service.
Mohammed et al. (2022)	Autonomous PV/battery system	Extended sizing, energy management, techno-economic optimization, and experimental validation	Optimized autonomous PV/battery operation	Strong component-level validation; less emphasis on field-surveyed village load and 25-year demand growth.
Quiles-Cucarella et al. (2023)	Household-scale standalone PV	Sequential Monte Carlo + particle-swarm optimization	9.9 kW PV and five 3.55 kWh batteries in case study	More advanced stochastic optimizer; much smaller scale than the present community system.
Lewis et al. (2024)	Kabuiri, northeast Nigeria; 610 kWh/day	HOMER PV–battery–generator optimization	LCOE 0.0927 USD/kWh; NPC USD 266,709	Closest Nigerian community benchmark; dispatchable generator reduces storage-only reliability risk.
Present study	Itunta, Nigeria; 806.16 kWh/day	Field survey + PVGIS + MATLAB stochastic lifecycle model	174.32 kWp; optimized 598 batteries; LCOE ₦358.63/kWh; Year-1 reliability 91.82% in lifecycle case	Adds PV-only long-term degradation, load growth, NPC, practical storage strategy, and explicit uncertainty screen.

3.15 Practical Implications, Limitations, and Transferability

The principal practical implication is that storage dominates both cost and operational risk. The optimized one-day design reduces capital burden, but it also increases dependence on accurate weather and demand forecasting, rapid maintenance response, and disciplined load management. The conservative three-day design provides additional resilience at a substantial cost premium. A staged approach is therefore recommended: commission the one-day modular configuration, reserve space and DC/inverter interfaces for expansion, monitor minimum SoC and ENS, and add PV or storage when predefined thresholds are reached.

The study has several limitations. The household profile is based on appliance inventory and reported operating hours rather than long-duration smart-meter measurements; the reliability model uses a daily time step; battery aging coefficients are scenario-based rather than calibrated to a specific cell chemistry and thermal enclosure; component prices and diesel costs are time-sensitive; and the model has not yet been replicated in HOMER or PVsyst. These limitations mean that the reported capacities and costs are planning estimates. They do not remove the value of the integrated framework, but they require detailed hourly simulation, vendor-specific design, and field monitoring before construction.

Transferability is therefore methodological rather than numerical. Other communities can apply the same sequence—field load survey, long-term resource characterization, deterministic pre-sizing, stochastic reliability testing, storage cost–reliability optimization,

lifecycle costing, and expansion planning—but must replace the Itunta load, climate, equipment, and financial assumptions with local data.

4. Conclusion

This study presents an integrated planning framework for a standalone PV mini-grid serving Itunta Village. The field survey established a baseline demand of 806.16 kWh/day, while the conservative design used 174.32 kWp of PV and three days of storage. The principal scientific contribution is the combined treatment of site-specific demand, stochastic and seasonal solar variability, battery cost–reliability optimization, lifecycle economics, and long-term adequacy under load growth. The technical sensitivity analysis showed that the average reserve margin is vulnerable to a 10% irradiance reduction or load increase, confirming that average-value sizing alone is insufficient.

The optimized one-day storage configuration reduces the battery bank from 896 to 598 units and lowers battery cost from approximately ₦516.09 million to ₦344.45 million while satisfying the adopted reliability constraints. The simplified LCOE is ₦89.91/kWh, whereas the discounted lifecycle LCOE is ₦358.63/kWh and the NPC is approximately ₦1.02 billion. Battery cost and replacement remain the dominant economic drivers. Under 2% annual load growth, lifecycle reliability declines from 91.82% in Year 1 to 54.26% in Year 25, and the 5% growth case deteriorates much faster. The system is therefore feasible for current demand but should be implemented as a modular plant with metering, thermal and safety controls, replacement funding, and a planned reinforcement window. Hourly commercial-software validation and vendor-specific battery-aging calibration are recommended before procurement.

Recommendation

i. **Adopt lifecycle-based economic evaluation:** Future mini-grid studies should report both simplified and discounted LCOE, because simplified cost estimates understate the effect of financing, inflation, and replacement.
ii. **Use optimized storage sizing where reliability targets permit:** The 1-day autonomy solution is the cost-reliability sweet spot for the present demand base while the 3-day design may be retained only where extra resilience is required.
iii. **Plan mid-life expansion:** Since reliability declines steadily over the project life, additional PV capacity, hybrid support or storage reinforcement should be scheduled between Years 10 and 15.
iv. **Use modular higher-voltage DC architecture:** Large systems should not rely on a single low-voltage bulk bus instead; they should use string grouping and MPPT-based regulation to keep current manageable and improve safety.
v. **Treat diesel benchmarks as conservative**: The 450 ₦/kWh value is a present-day reference point but it does not capture future escalation; policy comparisons should recognize that diesel life-cycle cost is likely higher over time.
vi. **Monitor reliability indicators continuously**: ENS, LPSP and battery state-of-charge should be tracked during operation to support adaptive load management and timely reinforcement.
vii. **Strengthen environmental and end-of-life planning:** Battery replacement, recycling, thermal management, and safe disposal should be integrated into implementation planning from the beginning.

List of Abbreviations

AC – Alternating Current
Ah – Ampere-hour
BoS – Balance of System
CAPEX – Capital Expenditure
DC – Direct Current
DoD – Depth of Discharge
ENS – Energy Not Served
EPBT – Energy Payback Time
EFC – Equivalent Full Cycle
HOMER – Hybrid Optimization of Multiple Energy Resources
LCOE – Levelized Cost of Electricity
NPC – Net Present Cost
LLP – Loss of Load Probability
LPSP – Loss of Power Supply Probability
MPPT – Maximum Power Point Tracking
NOCT – Nominal Operating Cell Temperature
O&M – Operation and Maintenance
OPEX – Operating Expenditure
PSH – Peak Sunshine Hours
PV – Photovoltaic
PVGIS – Photovoltaic Geographical Information System
RSM – Response Surface Methodology
SoC – State of Charge
SoH – State of Health
SPP – Simple Payback Period
SPR – Solar Performance Ratio
Wp – Watt-peak

–**Declarations**

Availability of data and materials

The authors declare that all data and materials used in this study were obtained from environmental weather archive of Itunta Village, from the Photovoltaic Geographical Information System (PVGIS). Technical specifications and cost data were sourced from manufacturers' data sheets and publicly available documentation. No financial or non-financial assistance was received from any organization or individual. All data and materials supporting the findings of this study are available from the corresponding author upon reasonable request.

Ethical approval

This study was approved by the Research Ethics Committee of Michael Okpara University of Agriculture, Umudike, Abia State, Nigeria (Approval No: MOUAU/REC/2024/012, dated 15 March 2024). The study was conducted in accordance with the Declaration of Helsinki.

Competing interests

The authors declare that there are no known financial or non-financial competing interests associated with this study.

Funding

The authors declare that no funding was received from any financial or non-financial organization or individual to conduct this research.

Clinical trial
Not applicable.
Consent to publish
Not applicable.
Consent to participate
Written informed consent was obtained from all participants before data collection. Participants were informed that participation was voluntary, they could withdraw at any time without penalty, and that all responses would be anonymised.
Authors' contributions
All authors contributed substantially to the conception, system design, simulation modelling, data analysis, interpretation of results, and manuscript preparation. All authors reviewed and approved the final manuscript.
Acknowledgements
The authors acknowledge the use of PVGIS and other open-access technical resources that supported the modelling and analysis of this work. Above all, gratitude is extended to God Almighty for the wisdom, strength, and good health granted throughout the course of this research.
Authors' information
The authors are researchers in the fields of renewable energy systems, power engineering, and sustainable infrastructure development, with academic and research interests focused on rural electrification, solar photovoltaic mini-grids, and long-term energy system reliability.

References

Adefarati, T., Bansal, R. C., Naidoo, R., Onaolapo, K. A., Bettayeb, M., Olulope, P. K., & Sobowale, A. A. (2024). Design and techno-economic assessment of a standalone photovoltaic-diesel-battery hybrid energy system for electrification of rural areas: A step towards sustainable development. Renewable Energy, 227, 120556. https://doi.org/10.1016/j.renene.2024.120556.

Al-Shetwi, A. Q. (2016). Design and economic evaluation of electrification of small villages in rural area in Yemen using stand-alone PV system. *International Journal of Renewable Energy Research (IJRER)*, *6*(1), 289-298.

Babatunde, O. M., Adedoja, O. S., Babatunde, D. E., & Denwigwe, I. H. (2019). Off-grid Hybrid Renewable Energy System for Rural Healthcare Centres: A Case Study in Nigeria. In *Energy Science & Engineering*. https://doi.org/10.1002/ese3.314.

Benchrifa, M., & Mabrouki, J. (2022). Simulation, sizing, economic evaluation and environmental impact assessment of a photovoltaic power plant for the electrification of an establishment. *Advances in Building Energy Research, 16*(6), 736–753. https://doi.org/10.1080/17512549.2022.2096693

Bhatia A. (2008). Design and Sizing of Solar Photovoltaic Systems. www.cedengineering.com.

Chanchangi, Y. N., Adu, F., Ghosh, A., Sundaram, S., & Mallick, T. K. (2023). Nigeria's energy review: Focusing on solar energy potential and penetration. *Environment, Development and Sustainability*, *25*(7), 5755–5796. https://doi.org/10.1007/s10668-022-02308-4.

Chandramouli, A., Sivachidambaranathan, V., & Arulmurugan, R. (2019). Modelling and design of a five-parameter single diode photovoltaic model with an artificial intelligence MPPT power system. *Nonlinearity*, *13*, 18.

Carabajal, A. T., Orsot, A., Moudio, M. P. E., Haggai, T., Okonkwo, C. J., Jarrard, G. T., III, & Selby, N. S. (2024). Social and economic impact analysis of solar mini-grids in rural Africa: A cohort study from Kenya and Nigeria. Environmental Research: Infrastructure and Sustainability, 4, 025005. https://doi.org/10.1088/2634-4505/ad4ffb.

Chen, Z., Xu, Y., Zhang, H., Guo, Y., & Zhang, X. (2023). Optimal design and performance assessment for a solar powered electricity, heating and hydrogen integrated energy system. *Energy, 262*, Article 125453. https://doi.org/10.1016/j.energy.2022.125453

Chetan S. S., (2014). Solar Photovoltaic Technology and Systems. PHI Leaning Private Limited: Delhi-110092.

Chidiebere Diyokea, Kenneth C. Ugwua, and Anthony C. Nnaji (2021). Techno-economic analysis of a grid-connected solar PV for a University Departmental Building in Enugu, Nigeria. International Journal of Scientific & Engineering Research Volume 12, Issue 8: 744 ISSN 2229-5518.

Cyril, A. O., Ujah, C. O., Ekwueme, B. N., & Asadu, C. O. (2024). Photovoltaic mini-grid incorporation: The panacea for electricity crisis in sub-Saharan Africa. *Unconventional Resources*, 100079.

Das, S. K., & Frank, D. (2019). Assessment of Various Parametric Effects on the Performance of a Commercial Grade Photovoltaic Solar Panel. In E3's Web of Conferences. https://doi.org/10.1051/e3sconf/201912202002.

Debnath, D., & Chatterjee, K. (2016). Neutral Point Clamped Transformerless Grid Connected Inverter Having Voltage Buck–boost Capability for Solar Photovoltaic Systems. In Iet Power Electronics. https://doi.org/10.1049/iet-pel.2014.0873.

Diyoke, C., Ngwaka, U., & Ugwu, K. (2023). A comprehensive analysis on the grid-tied solar photovoltaics for clean energy mix and supply in Nigeria's on-grid power. Journal of Energy Systems, 7(1), 1–17. https://doi.org/10.30521/jes.988844

Fakher Alfahed, R. K., Oudah, S., & Al-jabori, K. (2019). Electrification of a rural home by solar photovoltaic system in Haur Al-Hammar of Iraq. *Journal of Energy Management and Technology*, *3*(3), 30-40.

Gutiérrez-Martín, F., Díaz-López, J. A., Caravaca, A., & Dos Santos-García, A. J. (2024). Modeling and simulation of integrated solar PV-hydrogen systems. *International Journal of Hydrogen Energy, 52*, 995–1006. https://doi.org/10.1016/j.ijhydene.2023.05.179

Habib, S., Jia, Y., Tamoor, M., Zaka, M. A., Shi, M., & Dong, Q. (2023). Modeling, simulation, and experimental analysis of a photovoltaic and biogas hybrid renewable energy system for electrification of rural community. *Energy Technology, 11*(10), Article 2300474. https://doi.org/10.1002/ente.202300474

Jara, P. G., Castro, M. T., Esparcia, E. A., & Ocon, J. D. (2020). Quantifying the Techno-Economic Potential of Grid-Tied Rooftop Solar Photovoltaics in the Philippine Industrial Sector. In Energies. https://doi.org/10.3390/en13195070

Leonics (2009). Design of solar Photovoltaic system. https://www.leonics.com/support/article2_12j/articles2_12j_en.php.

Lewis, C. G., Ijeoma, M. W., Yakubu, R. O., Chukwu, B. N., Chen, H., & Carbajales-Dale, M. (2024). Achieving universal energy access in remote locations using HOMER energy model: A techno-economic and environmental analysis of hybrid microgrid systems for rural electrification in northeast Nigeria. Frontiers in Energy Research, 12, 1454281. https://doi.org/10.3389/fenrg.2024.1454281.

Luo, G., Zhang, Y., & Tang, A. (2023). Capacity degradation and aging mechanisms evolution of lithium-ion batteries under different operation conditions. Energies, 16(10), 4232. https://doi.org/10.3390/en16104232.

Li, N., Wang, J., & Zhang, Y. (2024). Design of small independent photovoltaic power generation system. In *Journal of Physics: Conference Series* (Vol. 2836, No. 1, p. 012002). IOP Publishing

Ma, J., & Yuan, X. (2023). Techno-economic optimization of hybrid solar system with energy storage for increasing the energy independence in green buildings. *Journal of Energy Storage, 61*, Article 106642. https://doi.org/10.1016/j.est.2023.106642

Mbinkar, E. N., Asoh, D. A., Tchuidjan, R., & Baldeh, A. (2021). Design of a photovoltaic mini-grid system for rural electrification in Sub-Saharan Africa. *Energy and Power Engineering*, *13*(3), 91-110.

Mohammed, C., Mohamed, M., Larbi, E. M., Manale, B., Hassan, Z., Jalal, B., & Zouggar, S. (2022). Extended method for the sizing, energy management, and techno-economic optimization of autonomous solar photovoltaic/battery systems: Experimental validation and analysis. *Energy Conversion and Management, 270*, Article 116267. https://doi.org/10.1016/j.enconman.2022.116267

Ngo, X. C., & Do, N. Y. (2022). The Impact of Electrical Energy Consumption on the Payback Period of a Rooftop Grid-Connected Photovoltaic System: A Case Study from Vietnam. International Journal of Renewable Energy Development, 11(2),

Quiles-Cucarella, E., Marquina-Tajuelo, A., Roldán-Blay, C., & Roldán-Porta, C. (2023). Particle swarm optimization method for stand-alone photovoltaic system reliability and cost evaluation based on Monte Carlo simulation. Applied Sciences, 13(21), 11623. https://doi.org/10.3390/app132111623.

Uwibambe, J. (2017). *Design of photovoltaic system for rural electrification in Rwanda* (Master's thesis, Universitetet i Agder; University of Agder).

Wassie, Y. T., & Adaramola, M. S. (2021). Socio-economic and environmental impacts of rural electrification with Solar Photovoltaic systems: Evidence from southern Ethiopia. *Energy for Sustainable Development*, 52-66. https://doi.org/10.1016/j.esd.2020.12.002.

Zhang, C., Xia, J., Guo, X., Huang, C., Lin, P., & Zhang, X. (2022). Multi-optimal design and dispatch for a grid-connected solar photovoltaic-based multigeneration energy system through economic, energy and environmental assessment. *Solar Energy, 243*, 393–409. https://doi.org/10.1016/j.solener.2022.08.016